Expression of LOX-1, an Oxidized Low-Density Lipoprotein Receptor, in Choroidal Neovascularization

Subfoveal choroidal neovascularization of various macular diseases is one of the causes of severe blindness, including age-related macular degeneration (AMD). Several environmental risk factors have been elucidated in the pathogenesis of AMD, including smoking,[1] atherosclerosis,[2] increased levels of plasma fibrinogen,[3] and low levels of antioxidant vitamins.[4] Recent observations support the hypothesis that antioxidant and/or vitamin treatment may delay progression of AMD and vision loss.[5] However, the exact cause of AMD remains to be determined.

Recently, Ikeda et al[6] showed that increased plasma oxidized low-density lipoprotein (oxLDL) levels may be involved in the pathogenesis of AMD. Oxidized LDL has been implicated as having a major role in atherosclerosis, and many of the pathologic and biochemical features seen in choroidal neovascularization are analogous to those seen in advanced atherosclerosis, such as the infiltration of monocytes and macrophages and the overexpression of adhesion molecules, monocyte chemotactic proteins, growth factors, and cytokines within lesions.[7,8] Lectinlike oxidized low-density lipoprotein receptor type 1 (LOX-1) is a recently identified oxLDL receptor that is abundantly expressed in vascular endothelial cells.[9] Its messenger RNA has been shown to be expressed in atheromatous lesions,[9] and LOX-1 up-regulation has been observed in several vascular lesions, including hypertensive remodeling lesions, diabetic vascular lesions, and macrophages.[10] The observation of LOX-1 up-regulation in vascular lesions, the potential roles of oxLDL in the pathogenesis of AMD, and the possible similarity between the pathogenesis of atherosclerosis and that of AMD prompted us to examine LOX-1 expression in choroidal neovascularization. In addition, we sought to measure plasma cholesterol levels to investigate the relationship between LOX-1 expression and hyperlipidemia.

We examined LOX-1 localization in 13 surgically excised neovascular membranes, including 10 from patients with AMD, 1 from a patient with idiopathic choroidal neovascularization, and 2 from patients with myopic choroidal neovascularization. The membranes were frozen in liquid nitrogen within 30 minutes of excision. Multiple 8-μm cryosections from each membrane were air-dried, fixed in acetone for 5 minutes, washed with phosphate-buffered saline, and blocked for 30 minutes with 2% bovine serum albumin in phosphate-buffered saline. They were then incubated with primary antibody and washed 3 times for 5 minutes with

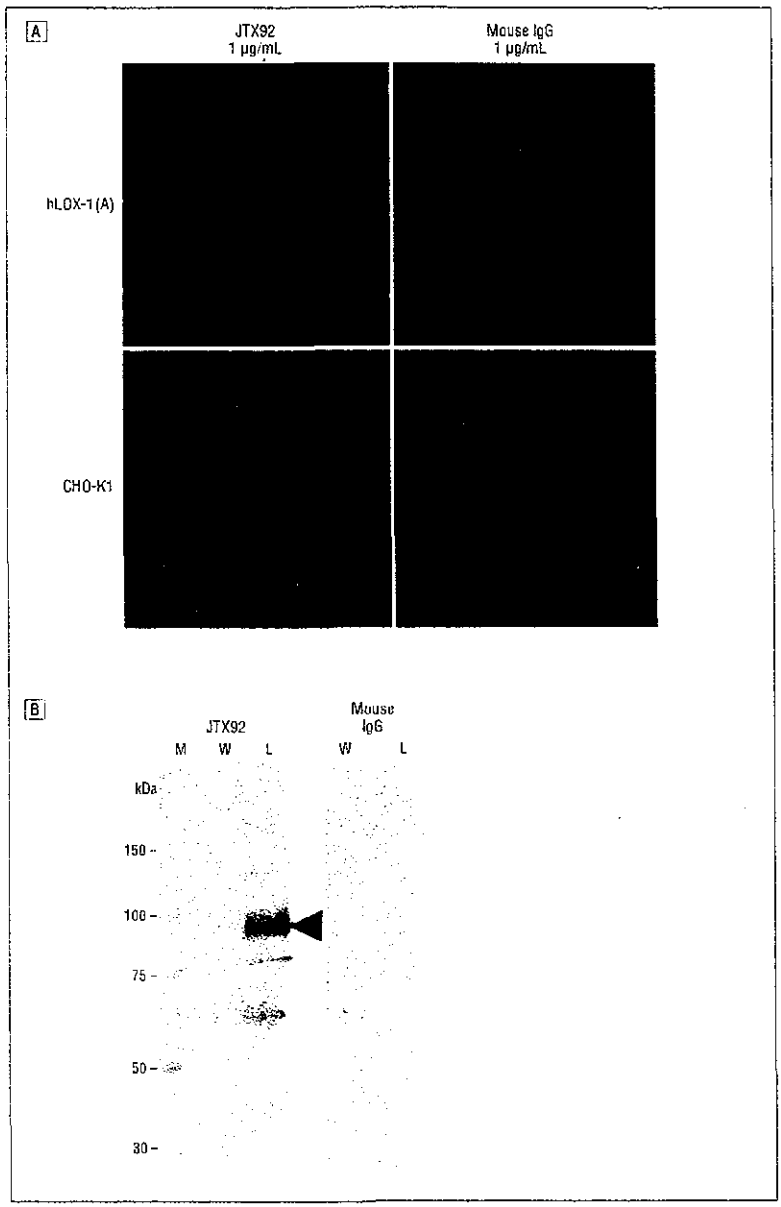

Figure 1. Immunostaining (A) and Western blot analysis (B) results of human lectinlike oxidized low-density lipoprotein receptor type 1 (LOX-1) complementary DNA (hLOX-1-CHO). A, Immunostaining of hLOX-1-CHO was performed. The nonfixed CHO cells were incubated with the primary antibody JTX92, then the bound antibody was detected with fluorescein isothiocyanate conjugated–antihuman IgG. B, Western blot analysis was performed to determine the specificity of the antibody. M indicates molecular weight marker; W, wild-type CHO cells; and L, CHO cells expressing hLOX-1. The arrowhead points to the expected molecular weight.

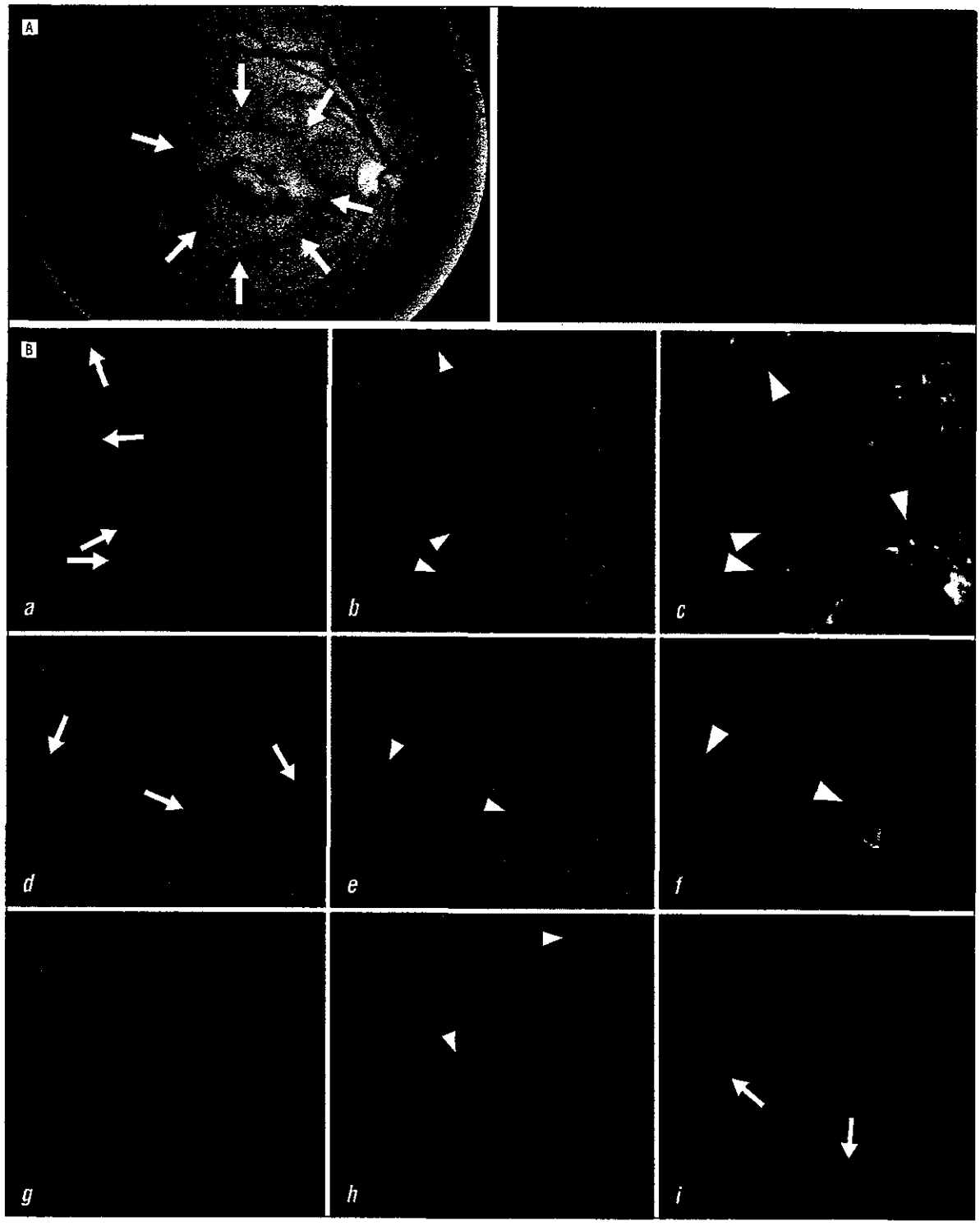

Figure 2. Fundus photograph and angiographic image (A) and immunostaining of surgically excised choroidal neovascular (CNV) membrane (B).
A, Representative color fundus photograph (left) and angiographic image (right) of the fundus of a 55-year-old man with age-related macular degeneration (patient 1). The area of serous retinal detachment is indicated by arrows. B, panels *a* through *i*, A CNV membrane from patient 1. Panels *a* and *d*, Lectinlike *oxidized* low-density lipoprotein receptor type 1 (LOX-1) staining is seen in red, some of which is indicated by arrows. Panels *b* and *e*, von Willebrand factor (vWF) staining for vascular endothelial cells is *seen in green*, some of which is indicated by small arrowheads. Panels *c* and *f*, Confocal image of double staining for LOX-1 and vWF. LOX-1 expression and vWF localization were associated, some of *which is indicated* by large arrowheads. Panel *g*, Control staining of a CNV membrane from patient 1. Panel *h*, image of double staining for LOX-1 and vWF for panel *g*. von Willebrand factor staining for *vascular endothelial* cells is seen in green, some of which is indicated by small arrowheads. Panel *i*, A CNV membrane from a 37-year-old woman with idiopathic CNV (patient 13). LOX-1 is faintly stained and seen in red, some of which is indicated by arrows. Panels *a* through *c*, original magnification ×200; *d* through *i*, original magnification ×600.

Table. Clinical and Histological Characteristics

Patient No./Eye/ Age, y/Sex	Diagnosis	TC, mg/dL (TC Status)	SRD, DD*	Preoperative CNV Size, DD†	LOX-1*	vWF*
1/L/55/M	AMD	229 (High)	3	1.0	+++	+++
2/R/57/M	AMD	202 (Normal)	2	0.8	+++	+++
3/L/73/F	AMD	282 (High)	1.5	0.8	++	++
4/L/80/M	AMD	291 (High)	1.2	0.7	++	++
5/R/89/M	AMD	226 (High)	1.5	0.5	++	+++
6/R/69/F	AMD	242 (High)	1.0	0.4	+	++
7/R/89/F	AMD	225 (High)	1.5	0.7	++	+
8/L/63/F	AMD	208 (Normal)	1.0	0.3	+	+
9/R/93/F	AMD	158 (Normal)	0.8	0.2	+	+
10/L/71/M	AMD	218 (Normal)	±	0.2	±	± - +
11/R/49/M	Myopic CNV	276 (High)	±	0.7	+	+
12/L/65/F	Myopic CNV	256 (High)	±	0.6	±	±
13/R/37/F	Idiopathic CNV	177 (Normal)	1.5	1.0	+	+

Abbreviations: AMD, age-related macular degeneration; CNV, choroidal neovascularization; DD, disk diameter; L, left; LOX-1, lectinlike oxidized low-density lipoprotein receptor type 1; R, right; SRD, serous retinal detachment; TC, total cholesterol level; vWF, von Willebrand factor.

SI conversion factor: To convert TC to millimoles per liter, multiply by 0.0259.

*Quantified by counting the number of LOX-1–positive vascular channels in multiples of 100 times the No. of objective fields. ± Indicates less than 1; +, 1 to 5; ++, 5 to 10; and +++, more than 10.

†Measured on fluorescein angiography.

phosphate-buffered saline. Bound antibody was detected with Cy3-biotin–conjugated secondary antibody. Polyclonal antibodies against human von Willebrand factor (DAKO Corp, Kyoto, Japan) were used to identify vascular endothelial cells. Antihuman LOX-1 monoclonal antibody (JTX92) was generated by immunizing BalbC/c mice with the CHO cell line that was transfected human LOX-1 complementary DNA (HLOX-1-CHO). Hybridomas from the splenocytes were prepared with the use of standard procedures and screened by means of the immunostaining of HLOX-1-CHO. The specificity of the antibody was determined by means of Western blot analysis and the immunostaining of HLOX-1-CHO (**Figure 1**). Immunohistochemical staining was repeated on cryosections of 10 choroidal neovascularization membranes, omitting the anti–LOX-1 primary antibody as controls. Additional control samples included immunohistochemical staining for LOX-1 of the posterior sclera, choroid, choriocapillaries, and retina of a normal donor eye.

The choroidal neovascular membranes ranged from moderately cellular with prominent neovascularization to paucicellular and fibrotic with few vascular channels. LOX-1 expression was detected in all, and most of the LOX-1 was localized to the endothelial cells (**Figure 2**). Staining for endothelial cells was seen in the LOX-1–positive cells. The LOX-1–positive profiles exceeded the number of von Willebrand factor–positive profiles, suggesting that LOX-1 was localized in nonvascular cells or within the stroma of neovascular membranes, as well as in the endothelial cells. The finding that the labeling of LOX-1 was not restricted to vascular endothelial cells is in line with recent observations in advanced atherosclerosis that LOX-1 is extensively expressed in the new blood vessels, macrophages, and smooth muscle cells of advanced atherosclerotic lesions.[10-12]

We did not find LOX-1 within the posterior segment of normal eyes, including the choriocapillaries (**Table**). As is further summarized in the Table, greater LOX-1 staining was found in the membranes of the patients with AMD compared with those with idiopathic or myopic choroidal neovascularization, those with a relatively high plasma total cholesterol level, and those of patients with larger macular serous detachment.

Our findings suggest that LOX-1 plays an active role in the pathogenesis of choroidal neovascularization, especially in AMD. However, further experiments are needed to determine whether LOX-1 plays a role in mediating the processes in AMD that are compatible with those in atherosclerosis.

Megumi Honjo, MD, PhD
Tatsuya Sawamura, MD, PhD
Junichi Hinagata, PhD
Kayo Nakamura, PhD
Nobuhito Sanada, PhD
Hidenobu Tanihara, MD, PhD
Yoshihito Honda, MD, PhD
Junichi Kiryu, MD, PhD

Correspondence: Dr Honjo (megumi@kuhp.kyoto-u.ac.jp).

Funding/Support: This study was supported in part by a Grant-in-Aid for Scientific Research from the Ministry of Education, Culture, Sports, Science, and Technology of Japan, Tokyo (Drs Honjo, Sawamura, Honda, and Kiryu), and by the Ministry of Health, Labor, and Welfare of Japan, Tokyo (Dr Sawamura).

1. Vingerling JR, Hofman A, Grobbee DE, de Jong PT. Age-related macular degeneration and smoking: the Rotterdam Study. *Arch Ophthalmol*. 1996; 114:1193-1196.
2. Friedman E. The role of the atherosclerotic process in the pathogenesis of age-related macular degeneration. *Am J Ophthalmol*. 2000;130: 658-663.
3. Smith W, Mitchell P, Leeder SR, Wang JJ. Plasma fibrinogen levels, other cardiovascular risk factors, and age-related maculopathy: the Blue Mountains Eye Study. *Arch Ophthalmol*. 1998;116:583-587.
4. Smith W, Mitchell P, Webb K, Leeder SR. Dietary antioxidants and age-related maculopathy: the Blue Mountains Eye Study. *Ophthalmology*. 1999;106:761-767.

5. Age-Related Eye Disease Study Research Group. A randomized, placebo-controlled, clinical trial of high-dose supplementation with vitamins C and E, beta carotene, and zinc for age-related macular degeneration and vision loss: AREDS report no. 8. *Arch Ophthalmol*. 2001;119:1417-1436.
6. Ikeda T, Obayashi H, Hasegawa G, et al. Paraoxonase gene polymorphisms and plasma oxidized low-density lipoprotein level as possible risk factors for exudative age-related macular degeneration. *Am J Ophthalmol*. 2001; 132:191-195.
7. Penfold PL, Madigan MC, Gillies MC, Provis JM. Immunological and aetiological aspects of macular degeneration. *Prog Retin Eye Res*. 2001; 20:385-414.
8. Oh H, Takagi H, Takagi C, et al. The potential angiogenic role of macrophages in the formation of choroidal neovascular membranes. *Invest Ophthalmol Vis Sci*. 1999; 40:1891-1898.
9. Sawamura T, Kume N, Aoyama T, et al. An endothelial receptor for oxidized low-density lipoprotein. *Nature*. 1997;386:73-77.
10. Nagase M, Abe J, Takahashi K, Ando J, Hirose S, Fujita T. Genomic organization and regulation of expression of the lectin-like oxidized low-density lipoprotein receptor (LOX-1) gene. *J Biol Chem*. 1998;273:33702-33707.
11. Li DY, Chen HJ, Staples ED, et al. Oxidized low-density lipoprotein receptor LOX-1 and apoptosis in human atherosclerotic lesion. *J Cardiovasc Pharmacol Ther*. 2002;7:147-153.
12. Kataoka H, Kume N, Miyamoto S, et al. Expression of lectinlike oxidized low-density lipoprotein receptor-1 in human atherosclerotic lesion. *Circulation*. 1999;99:3110-3117.

Histopathology of Documented Growth in Small Melanocytic Choroidal Tumors

Differentiation of a choroidal nevus from a small choroidal melanoma can be difficult. Choroidal nevi are generally asymptomatic lesions[1] that are less than 6 mm in diameter and less than 1.5 mm in height. The presence of drusen or areas of atrophy of the overlying retinal pigment epithelium generally indicate a *chronic, inactive* choroidal nevus.[1] Orange pigment and subretinal fluid are more commonly present in choroidal melanomas.[2] Echography usually demonstrates medium to high internal reflectivity in nevi and low reflectivity in melanomas. Documented growth[3,4] is widely interpreted as evidence of malignancy.

We provide the histopathology of 2 small choroidal melanocytic tumors that became symptomatic, developed orange pigment, and showed documented growth. One lesion was an epithelioid malignant melanoma; the other was a *benign nevus*.

Report of Cases. *Case 1.* A 45-year-old man was examined in May 1996 at the Ocular Oncology Clinic of the University of Michigan Kellogg Eye Center, Ann Arbor, for an enlarging, small juxtapapillary choroidal lesion in his right eye. A photograph from 1994 (**Figure 1**) showed a flat, brown 3.0×1.8-mm choroidal lesion, superior to the disc, without drusen or orange pigment. The lesion had increased to 3.0×3.0 mm and developed extensive orange pigment over its surface. Echography revealed a maximal height of 1.5 mm with a medium internal acoustic pattern. The initial diagnosis was a probable melanoma, but a decision was made to observe for evidence of continued growth before initiating therapy. In July 1996, the patient complained of blurred vision in his right eye. Results of an examination showed that the base had further increased to 3.3×3.2 mm (**Figure 2**). Repeat echography revealed that tumor height had

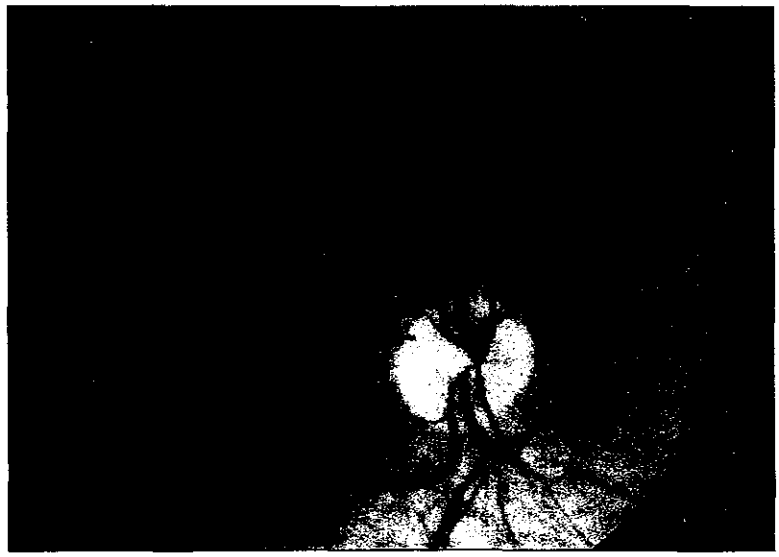

Figure 1. Fundus photograph of the right eye of case 1 shows a flat, pigmented choroidal lesion superior to the disc.

Figure 2. Fundus photograph of the right eye of case 1 shows a symptomatic, enlarged choroidal lesion 2 years after the photograph in Figure 1.

Dynamin-2 Regulates Oxidized Low-Density Lipoprotein–Induced Apoptosis of Vascular Smooth Muscle Cell

Yuji Kashiwakura, MD, PhD; Masami Watanabe, MD, PhD; Norihiro Kusumi, MD; Katsuhiko Sumiyoshi, PhD; Yasutomo Nasu, MD, PhD; Hiroshi Yamada, PhD; Tatsuya Sawamura, MD, PhD; Hiromi Kumon, MD, PhD; Kohji Takei, PhD; Hiroyuki Daida, MD, PhD

Background—On exposure to oxidized low-density lipoprotein (oxLDL), vascular cells generally undergo apoptosis, which is one of the major pathogenic factors of atherosclerosis. In this study, we examined the role of dynamin (a crucial GTPase protein in endocytosis) in oxLDL-induced apoptosis of vascular smooth muscle cells (VSMC).

Methods and Results—After oxLDL stimulation, dynamin-2 colocalized with LOX-1 around the cell surface, as well as oxLDL in the cytoplasm, suggesting that dynamin-2 was involved in scavenger receptor–mediated oxLDL endocytosis. Downregulation of dynamin-2 induced by dynamin-2 dominant negative plasmid (K44A) resulted in a decrease of oxLDL uptake and thereby in a reduction of apoptosis. These data demonstrated that dynamin-2 was involved in oxLDL-induced apoptosis via the oxLDL endocytotic pathway. On the other hand, dynamin-2 wild-type plasmid transfection promoted oxLDL-induced apoptosis without increasing oxLDL uptake. Interestingly, the p53 inhibitor pifithrin-α (PFT) significantly reduced apoptosis promoted by wild-type dynamin-2 (78% reduction compared with the PFT[−] condition). These results indicated that dynamin-2 enhanced oxLDL-induced apoptosis of VSMC by participating in the p53 pathway, probably as a signal transducer. Moreover, we demonstrated that, in advanced plaques of apolipoprotein $E^{-/-}$ mice, dynamin-2 expression was often enhanced in apoptotic VSMC, suggesting that dynamin-2 might participate in apoptosis of VSMC even in vivo.

Conclusions—Our data demonstrated that dynamin-2 at least partially regulated oxLDL-induced apoptosis of VSMC by participating in 2 independent pathways: the oxLDL endocytotic pathway and the p53 pathway. These findings suggest that dynamin-2 may serve as a new research or therapeutic target in vascular disease. **(*Circulation*. 2004;110:3329-3334.)**

Key Words: apoptosis ■ atherosclerosis ■ lipoproteins ■ cells, muscle, smooth

Apoptosis is a prominent feature in atherosclerotic lesions of humans and experimental animals and can affect macrophages, T lymphocytes, endothelial cells, and vascular smooth muscle cells (VSMC). Oxidized low-density lipoprotein (oxLDL) is one of the major atherogenic substances that induce apoptosis in many types of cells.[1–4] The mechanism of oxLDL-induced apoptosis probably varies among cell types. In macrophages, oxLDL activates tumor suppressor p53 and manganese superoxide dismutase, which are responsible for apoptosis.[5] In endothelial cells, the ceramide pathway or Fas-mediated pathway has been thought to mainly contribute to apoptosis.[3,6] Recent studies on human atherosclerotic lesions and aneurysms revealed that p53 or Fas antigen could be detected in apoptotic VSMC of diseased vessels.[7] However, most of the mechanisms that induce apoptosis in oxLDL-stimulated VSMC remain unknown.

Dynamin is a 100-kDa GTPase that is thought to pinch off vesicles from the plasma membrane at the fission step and is normally present in the cytosol as dimers or tetramers.[8] Dynamin-1 and dynamin-3 are considered to be neuron- and testis-specific isoforms, respectively, whereas dynamin-2 is reported to be ubiquitous.[9] During various types of endocytosis processes such as clathrin-coated pit endocytosis, caveolar endocytosis, and phagocytosis, dynamin likely assembles into a ringlike structure around the neck of the bud, where it functions directly or indirectly in pinching off vesicles from the plasma membrane.[10]

It has been demonstrated already that native LDL is internalized into the endosome via clathrin-coated pit endocytosis involving dynamin.[11] However, no study has directly demonstrated the involvement of dynamin in oxLDL endocytosis even though it has been elucidated that

Received March 23, 2004; de novo received May 15, 2004; revision received June 30, 2004; accepted July 6, 2004.

From the Department of Cardiology, Juntendo University School of Medicine, Tokyo (Y.K., K.S., H.D.); Departments of Urology (M.W., N.K., Y.N., H.K.) and Neuroscience (H.Y., K.T.), Okayama University Graduate School of Medicine and Dentistry, Okayama; and National Cardiovascular Center Research Institute, Osaka (T.S.), Japan.

Correspondence to Yuji Kashiwakura, MD, PhD, Department of Cardiology, Juntendo University School of Medicine, 2-1-1 Hongo, Bunkyo-ku, Tokyo 113-8421, Japan. E-mail yu-kashi@med.juntendo.ac.jp

Circulation is available at http://www.circulationaha.org

DOI: 10.1161/01.CIR.0000147828.86593.85

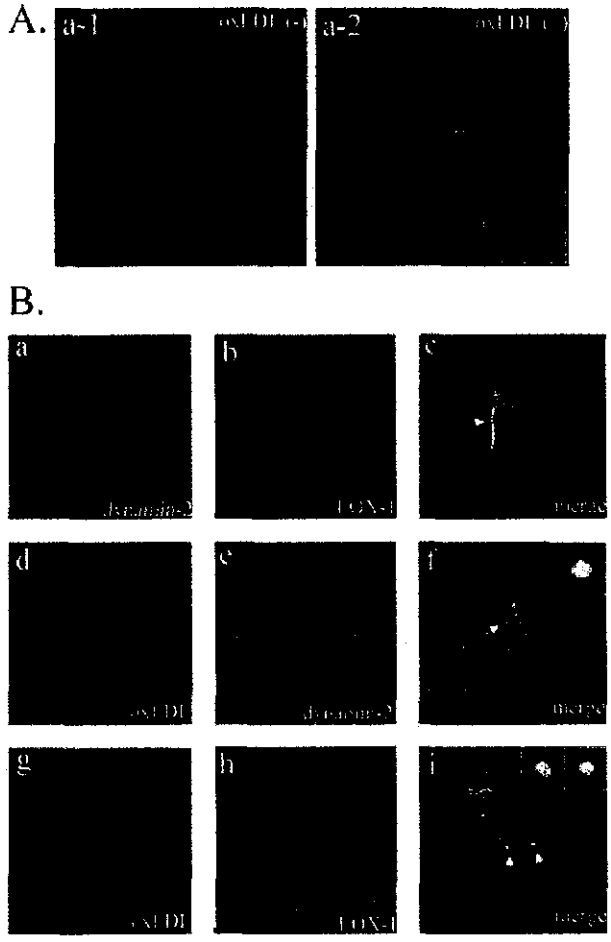

Figure 1. A, Confocal microscopy of immunostained (dynamin-2) VSMC under normal conditions (a-1) and oxLDL-stimulated conditions (a-2). After 1 hour of oxLDL stimulation, immunostaining with dynamin-2 antibody was performed in VSMC. After oxLDL stimulation, dynamin-2 shifted to the cell surface and could be detected as dots in a-2 (in frame). Magnification ×400. B, Confocal microscopy of double-stained VSMC (dynamin-2, LOX-1, and oxLDL). One hour after unlabeled oxLDL stimulation, double immunostaining of VSMC was performed. LOX-1 colocalized with dynamin-2 on the cell surface, indicated by arrow in c. Forty-five minutes after DiI-labeled oxLDL stimulation, an immunocytochemical study with the use of dynamin-2 or LOX-1 antibody was performed in VSMC. Dynamin-2 or LOX-1 colocalized with oxLDL in the cytoplasm in addition to around the cell surface. Arrow in f or i indicates colocalization of dynamin-2 and DiI-labeled oxLDL or LOX-1 and DiI-labeled oxLDL in the cytoplasm, respectively. Zoomed images of colocalization are shown in the right top corner of f and i. Magnification ×400.

CD36 and LOX-1 internalize into endosome via caveolar endocytosis (clathrin independent) or probably clathrin-coated pit endocytosis, respectively.[12] Recently, however, evidence that dynamin-2 is involved in apoptosis has been reported gradually.[13,14] However, there has been no study on the involvement of dynamin in apoptosis of vascular cells.

In the present study, we first attempted to validate the involvement of dynamin-2 in oxLDL uptake by VSMCs and then investigated the role of dynamin-2 in VSMC apoptosis.

Methods

Cells and Cell Culture

Primary human coronary smooth muscle cells (CASMC, Chambrex) were cultured in the recommended culture medium (SmGM-2, Chambrex) containing 1% penicillin/streptomycin and other supplemented growth factors. VSMC of passages 3 to 7 were used in all experiments.

Immunocytochemistry

Cells grown in 8-well chamber slides for 2 days were washed with PSB 3 times and then fixed with 4% paraformaldehyde for 60 minutes at 4°C and permeabilized with 0.1% Triton X-100 (Sigma) before exposure to the primary antibody. Cells were exposed to blocking solution (Blockace, Yukijirushi) for 2 hours at 4°C and then to the first antibody for 1 hour at room temperature. The bound first antibody was detected with the use of the respective second antibody. Normal staining of dynamin-2 or double staining of dynamin-2 and LOX-1 in VSMC was performed 1 hour after oxLDL stimulation with the use of dynamin-2 (goat polyclonal, Santa Cruz) and/or LOX-1 (rabbit polyclonal, Santa Cruz) antibody. Second antibody for dynamin-2 or LOX-1 was Texas red–conjugated anti-goat antibody (Jackson Labs) or FITC-conjugated anti-rabbit antibody (Jackson Labs).

Preparation of DiI-Labeled OxLDL

We obtained oxLDL (90% to 100% oxidation) from Intracell Corp. With the use of 1,1′-dioctadecyl-3,3,3′,3′-tetramethylindocarbocyanine perchlorate (DiI) (Molecular Probes), labeling of oxLDL was done basically as previously described.[15]

Plasmid (WDp or K44A) and Transfection

The cells were seeded in 8-well chamber slides at a density of 1×10^5 cells per well, incubated for 24 hours, and then transfected with the respective plasmid (dynamin-2 wild-type cDNA/GFP fusion plasmid [WDp/GFP], dynamin-2 dominant negative/GFP fusion plasmid [K44A/GFP], or control GFP plasmid [EGFP-N1, original plasmid of WDp/GFP and K44A/GFP, Clontec])[14] by lipofection (Invitrogen). Both the transfection efficiency and the levels of transgene expression of 3 types of plasmids in VSMC were almost the same (data not shown).

OxLDL Uptake of Plasmid (WDp/GFP or K44A/GFP)-Transfected Cells

After 24 hours of plasmid transfection, DiI-labeled oxLDL (5 μg/mL) was added to the culture medium of transfected cells. After incubation for 6 hours with oxLDL under serum-starved conditions, the cells were washed 5 times with PBS and then fixed with 4% paraformaldehyde in PBS for 30 minutes. Thereafter, DiI-fluorescent intensity of each of GFP-positive cells was determined by fluorescent microscope with the use of Meta imaging software version 6.1 (Universal Image Corporation). After the setting of consistent intensity threshold, the integrated intensity of each cell was measured.

TUNEL Assay to Detect OxLDL-Induced Apoptosis

After 24 hours of transfection, oxLDL (50 μg/mL) was added to the culture medium, and 12 hours after oxLDL stimulation under serum-starved conditions, terminal deoxynucleotidyl transferase–mediated dUTP biotin nick-end labeling (TUNEL) assay was performed. In brief, the oxLDL-stimulated cells were washed twice with PBS and fixed with 4% paraformaldehyde at room temperature for 30 minutes. The fixed cells were washed and permeabilized in 0.1% Triton X-100 (Sigma) in PBS for 3 minutes at room temperature. Finally, the cells were washed and stained with the use of the In Situ Cell Death Detection Kit (TMR-red, Roche). To investigate the role of p53 in dynamin-2–related apoptosis, pifithrin-α (PFT) (50 nmol/L, Calbiochem), a p53 inhibitor, was treated in plasmid-

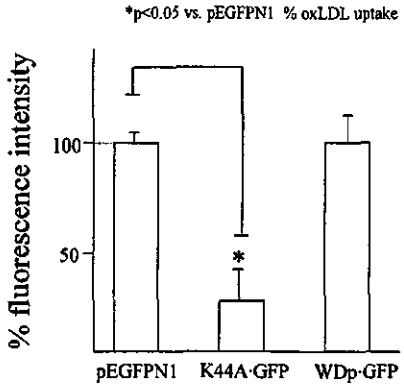

Figure 2. OxLDL uptake among the respective plasmid-transfected cells. After 6 hours of oxLDL stimulation, oxLDL uptake by K44A/GFP- or WDp/GFP-transfected cells was determined as described in Methods. White bar indicates percent fluorescence intensity. Lane 1: control pEGFPN1-transfected cells (percent fluorescence intensity=100); lane 2, K44A/GFP-transfected cells; lane 3, WDp/GFP-transfected cells. We measured the integrated intensity of a GFP-positive cell and calculated the average integrated intensity of 30 cells in each cell type in 1 experiment. We performed 5 independent experiments and analyzed statistically significant differences between subjects by Mann-Whitney *U* test. Differences were considered significant at $P<0.05$. Data are mean and SD of a representative experiment.

transfected cells for 12 hours before and with oxLDL stimulation, followed by TUNEL assay.

Animals

Male apolipoprotein E (apoE)$^{-/-}$ mice (aged 10 weeks; C57bl/6 background) and control C57bl/6 mice were obtained from Jackson Labs. All animal work was approved by regulatory authority of Juntendo University and performed in compliance with Japanese government guidelines.

Double Immunostaining With TUNEL of Aortic Cross Section

We prepared aortic cross sections of both control and apoE$^{-/-}$ mice 10 weeks after Western diet, as previously described.[16] Immunostaining was performed with the use of dynamin-2 and α-smooth muscle actin[17] (mouse, Biomeda) antibodies following the TUNEL procedure, as previously described.[18] In brief, the sample was fixed with 4% paraformaldehyde for 60 minutes at room temperature and permeabilized with 0.1% Triton X-100 (Sigma) for 5 minutes at room temperature. For TUNEL assay, the sample was incubated with a reaction mixture containing the enzyme terminal deoxynucleotidyl transferase and biotinylated dNTP nucleotides (Treviegen) for 1 hour at 37°C and then incubated with 2 first antibodies (dynamin-2 and α-smooth muscle actin) overnight at 4°C. Next, the sample was reacted with streptavidin Alexa Fluor 647 (Molecular Probes) together with both second antibodies tagged with Alexa Fluor 555 (anti-goat/rabbit, Molecular Probes) or Alexa Fluor 488 (anti-mouse/donkey, Molecular Probes). Additionally, we verified that the secondary antibodies did not recognize each other in control experiments.

Double staining (dynamin-2 and p53) was also performed with the use of p53 first antibody (rabbit, polyclonal, Chemicon) and anti-rabbit/donkey Alexa Fluor 488 secondary antibody (Molecular Probes).

Results

On exposure to oxLDL, various molecules become activated and participate in oxLDL-induced apoptosis of vascular cells.

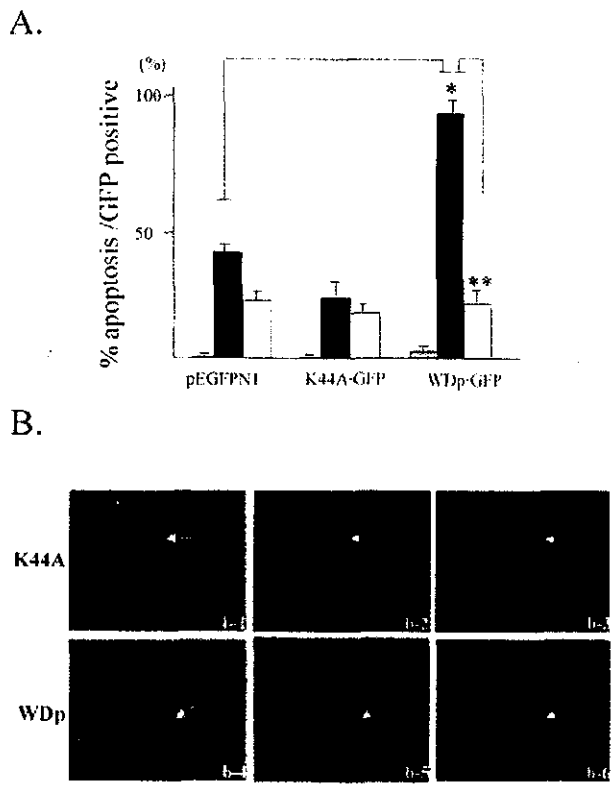

Figure 3. A, OxLDL-induced apoptosis of VSMC and effect of PFT, a p53 inhibitor, on apoptosis among K44A/GFP- or WDp/GFP plasmid-transfected cells. Three types of bars (slashed, black, white) indicate percentage of GFP-positive apoptotic cells per total number of GFP-positive cells in the respective plasmid-transfected cells under the following conditions in the absence of serum: slashed bar, oxLDL(−) condition; black bar, oxLDL(+) condition; white bar, PFT (50 nmol/L) treatment with oxLDL(+) condition. In total, we counted 100 GFP-positive cells in respective plasmid-transfected cells and calculated percentage of apoptotic cells per GFP-positive cells in 1 experiment. We performed 5 independent experiments and analyzed statistically significant differences between subjects by Mann-Whitney *U* test. Differences were considered significant at $P<0.05$. Data are mean and SD of a representative experiment. *$P<0.05$ vs pEGFPN1 % apoptosis; **$P<0.05$ vs WDp/GFP PFT(−) % apoptosis. B, Microscopic detection of nonapoptotic or apoptotic VSMC in K44A/GFP- or WDp/GFP-transfected cells under oxLDL stimulation. Plain phase: b-1 and b-4. GFP phase: b-2 and b-5. TUNEL phase: b-3 and b-6. Arrow indicates nucleus of K44A/GFP- or WDp/GFP-transfected cells. In b-1, b-2, b-3, arrow indicates nucleus of a typical nonapoptotic cell among K44A/GFP-positive cells. In b-4, b-5, b-6, arrow indicates nucleus of a typical apoptotic cell among WDp/GFP-positive cells. Magnification ×100.

In this study we investigated the role of dynamin-2 in oxLDL-induced apoptosis of VSMC, focusing especially on its participation in oxLDL endocytotic pathways and cell cycle pathways. Before all investigations, we preliminarily characterized the primary VSMC used in this study in regard to the expression pattern of 3 dynamin isotypes or several oxLDL receptors. VSMC expressed dynamin-2 but neither dynamin-1 nor dynamin-3. We could detect CD36, LOX-1, and SR-BI, but not SR-A, in VSMC and also confirmed that CD36 and LOX-1 were mainly responsible for oxLDL uptake in VSMC by competition assays

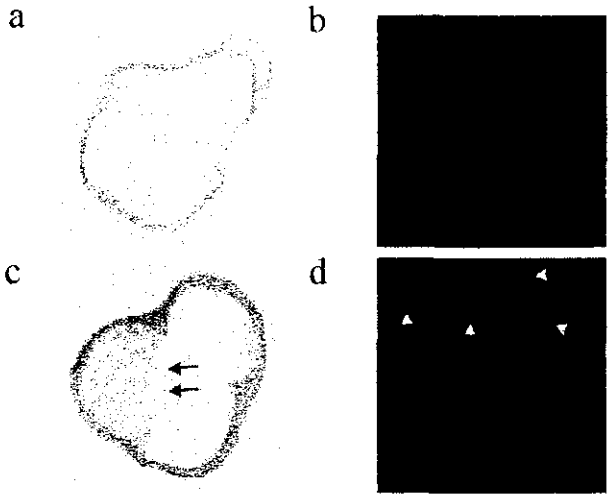

Figure 4. Dynamin-2 immunostaining of serial cross sections of supravalvular aorta of control and apoE$^{-/-}$ mice. a, Hematoxylin-eosin staining of control mouse. b, Immunostaining (dynamin-2) of media of control mouse. c, Hematoxylin-eosin staining of apoE$^{-/-}$ mouse. d, Immunostaining (dynamin-2) of plaque of apoE$^{-/-}$ mouse. A typical advanced plaque is shown in c (arrows). Immunostaining revealed that there was a population of cells that strongly expressed dynamin-2 in advanced plaque (d, arrows).

using blocking antibodies of CD36 (BD Pharmingen), LOX-1 (JTX92),[19] and SR-B (CLA-1, Novus Biologicals). After these preliminary experiments, we performed all other investigations.

The immunocytochemical study demonstrated that normally dynamin-2 distributed homogeneously in the cytoplasm (Figure 1A, a-1), whereas on oxLDL stimulation dynamin-2 shifted to the cell surface (a-2) and colocalized there with LOX-1 (Figure 1B, c, arrow). Moreover, dynamin-2 and LOX-1 colocalized with Dil-labeled oxLDL in the cytoplasm in addition to around the cell surface (Figure 1B, f and i, arrows), indicating that dynamin-2 and LOX-1 were incorporated into early endosomes together with oxLDL. We confirmed that dynamin-2 also colocalized with CD36 (data not shown). These data indicated that dynamin-2 was involved in scavenger receptor–mediated oxLDL endocytosis. Next, we investigated oxLDL uptake by VSMC where dynamin-2 was modulated. Twenty-four hours after transfection to VSMC with either WDp/GFP, K44A/GFP, or control GFP plasmid, Dil-labeled oxLDL uptake by VSMC was attempted. K44A/GFP transfection decreased oxLDL uptake significantly, whereas WDp transfection had no influence on oxLDL uptake (Figure 2). These results demonstrated that downregulation of dynamin-2 directly affected oxLDL uptake, although dynamin-2 overexpression alone could not enhance oxLDL endocytosis. On the basis of these findings, we concluded that dynamin-2 was one of the essential factors of oxLDL endocytosis.

Next, we investigated oxLDL-induced apoptosis in VSMC where dynamin-2 was modulated. Twenty-four hours after transfection with the respective plasmid, oxLDL stimulation (50 μg/mL) was performed for 12 hours to induce apoptosis, followed by TUNEL assay. Apoptosis was hardly detected in the absence of oxLDL in the 3 types of GFP-positive cells (Figure 3A, slashed bars). Among the control GFP-positive cells, the frequency of apoptosis was 42% (Figure 3A, lane pEGFPN1, black bar). Apoptotic cells were recognized much less frequently among K44A/GFP-positive cells (Figure 3B; top panels show a typical nonapoptotic cell) than among control GFP-positive cells (Figure 3A, black bar, 24% versus 42%). Given the previous report that K44A, a mutant defective GTP binding, could work as dominant negative in endocytotic pathways but not in apoptotic pathways,[13] the inhibition of apoptosis was probably due solely to the decrease of oxLDL uptake. Our data suggested that dynamin-2 downregulation reduced oxLDL-induced apoptosis by decreasing oxLDL uptake, which meant that dynamin-2 was involved in oxLDL apoptosis of VSMC via oxLDL endocytotic pathway. On the other hand, apoptosis could be detected more frequently among WDp/GFP-positive cells (Figure 3B; bottom panels show a typical apoptotic cell) than among control GFP-positive cells (Figure 3A, black bar, 93% versus 42%) even though there was no difference in the amount of oxLDL uptake between the 2 types of cells (Figure 2). In short, an increase of wild-type dynamin-2 did not affect oxLDL endocytosis but led to the promotion of apoptosis. These results suggested that on exposure to oxLDL, dynamin-2 also participated in some pathway related to apoptosis, besides the oxLDL endocytotic pathway.

To identify such an interesting pathway, we examined the effect of the p53 inhibitor PFT on apoptosis of cells overexpressing dynamin-2. After treatment with PFT (50 nmol/L) for 12 hours, oxLDL was added to the culture medium, followed by TUNEL assay. The results showed that PFT significantly reduced apoptosis of WDp/GFP-transfected cells by 78%, whereas it reduced apoptosis of control GFP-positive cells by only 45% (Figure 3A, white bars). As a result of PFT treatment, the final percentage of apoptotic WDp/GFP-transfected cell was almost the same as that of apoptotic control cells (≈20%). These data indicated that the p53 pathway might be mainly responsible for the apoptosis promoted by overexpressed dynamin-2. We speculated that the apoptosis observed despite treatment with PFT was mediated through pathways different from the p53 pathway.[7] We also performed the same experiments using Fas ligand neutralizing antibodies or tumor necrosis factor-α receptor I and II neutralizing antibodies. These results showed that both blocking antibodies could not reduce the percentage of apoptotic cells among WDp-transfected cells to that in control cells (data not shown), suggesting that dynamin-2 is not likely to be involved in either Fas/Fas ligand or in the TNF-α–mediated apoptotic pathway. Our findings suggested that dynamin-2 promoted oxLDL-induced apoptosis by participating only in the p53 pathway.

We also investigated in vivo dynamin-2 expression in advanced plaque in serial cross sections of the aorta from apoE$^{-/-}$ mice (Figure 4c; arrows indicate advanced plaque) and control mice (Figure 4a; no intima). Immunostaining

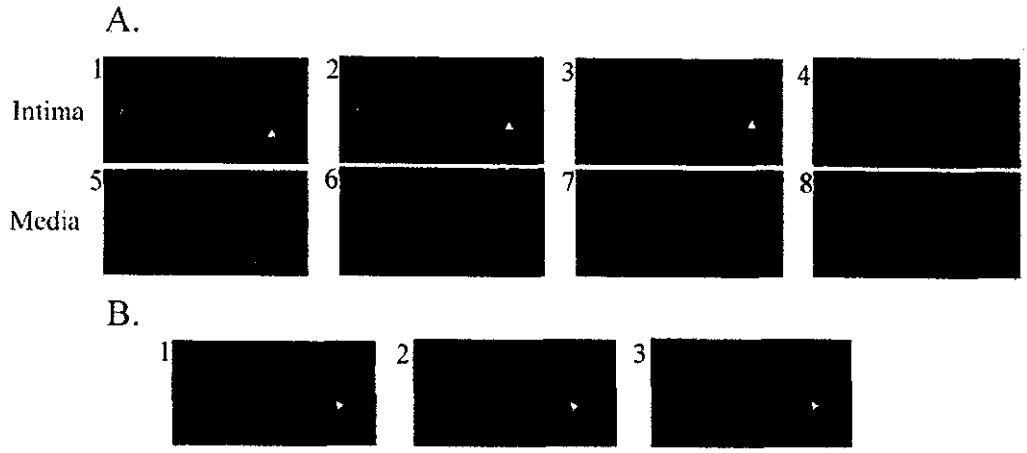

Figure 5. A, Double staining (dynamin-2 and α-smooth muscle actin) with TUNEL assay of sections adjacent to the samples in a or c of Figure 4. 1 to 4: cells in the advanced plaque. 5 to 8: cells in the media. α-Smooth muscle actin phase: 1 and 5. Dynamin-2 phase: 2 and 6. TUNEL phase: 3 and 7. DAPI phase: 4 and 8. In panels 1, 2, and 3, white or green arrow indicates an apoptotic VSMC overexpressing dynamin-2 or nonapoptotic VSMC, respectively. Magnification ×100. B, Double staining (dynamin-2 and p53) with TUNEL assay of sections adjacent to the sample shown in c of Figure 4. 1: dynamin-2 phase. 2: TUNEL phase. 3: p53 phase. Arrow indicates an apoptotic cell overexpressing dynamin-2 positive for p53. The frequency of p53- or dynamin-2–positive apoptotic cells was ≈21.1% or 3.6% of total apoptotic cells, respectively. The average frequency of double-positive cells per total apoptotic cells was 3.6%.

demonstrated that there was a population of cells that strongly expressed dynamin-2 (Figure 4d; arrow) in the advanced plaque but not in the media (Figure 4b). Double staining with TUNEL assay revealed that the average frequency of apoptosis in intimal cells (5 mice) was 2.8% (range, 0.6% to 5.4%). Interestingly, dynamin-2 expression was often enhanced in apoptotic VSMC (Figure 5A, 1 to 4; white arrow indicates dynamin-2–positive apoptotic VSMC). Moreover, p53 expression could be detected in several apoptotic cells overexpressing dynamin-2 (Figure 5B, arrow), implicating the participation of dynamin-2 in the p53 pathway in vivo. One sixth of p53-positive apoptotic vascular cells were dynamin-2 positive, whereas all dynamin-2–positive apoptotic cells were p53 positive. Given these quantitative results, dynamin-2 may play an additional rather than an essential role in the p53-dependent apoptotic pathway. Recently, several studies demonstrated abnormalities of endocytosis-related proteins such as dynamin in some diseases. For instance, a correlation has been reported between dynamin-related protein abnormalities and inherited optic neuropathy.[20] However, no study has analyzed atherosclerosis from the viewpoint of dynamin. Our data suggest that dynamin-2 might be involved in apoptosis of intimal migratory cells, even in vivo.

Discussion

The mechanism by which dynamin-2 is involved in the apoptotic pathway has been explored only minimally. Dynamin-2 has been shown to interact with several signaling molecules such as ERK kinase and grb2.[21,22] We speculate that dynamin governs membrane dynamics at the cell surface to thereby activate the p53-dependent apoptotic cascade. It has been demonstrated that inhibition of Rac, a member of the Rho superfamily, elicits a p53-dependent apoptotic response.[23] Interestingly, dynamin has been reported to translocate Rac from the cell surface to the perinucleus and then deactivate Rac by inversing Rac-GTP to Rac-GDP.[24] Given these reports, dynamin-2 may participate in the p53-dependent pathway by modulating Rac localization and activity.

In conclusion, our data demonstrated that dynamin-2 at least partially regulated oxLDL-induced apoptosis of VSMC by participating in at least 2 independent pathways: the oxLDL endocytotic pathway and the p53 pathway. These findings suggest that dynamin-2 may serve as a new research or therapeutic target in vascular disease.

References

1. Hardwick SJ, Hegyi L, Clare K, et al. Apoptosis in human monocyte-macrophage exposed to oxidized low-density lipoprotein. *J Pathol.* 1996; 179:294–302.
2. Escargueil-Blanc I, Salvayre R, Negre-Salvayre A. Necrosis and apoptosis induced by oxidized low density lipoprotein occur through two calcium-dependent pathways in lymphoblastoid cells. *FASEB J.* 1994;8: 1075–1080.
3. Harada-Shiba M, Kinoshita M, Kamido H, et al. Oxidized low density lipoprotein induces apoptosis in cultured human umbilical vein endothelial cells by common and unique mechanisms. *J Biol Chem.* 1998;273: 9681–9687.
4. Jovinge S, Crisby M, Thyberg J, et al. DNA fragmentation and ultrastructural changes of degenerating cells in atherosclerotic lesions and smooth muscle cells exposed to oxidized LDL in vitro. *Arterioscler Thromb Vasc Biol.* 1997;17:2225–2231.
5. Kinscherf R, Claus R, Wanger M, et al. Apoptosis caused by oxidized LDL is manganese superoxide dismutase and p53 dependent. *FASEB J.* 1998;12:461–467.
6. Sata M, Walsh K. Oxidized LDL activates Fas-mediated endothelial cell apoptosis. *J Clin Invest.* 1998;102:1682–1682.
7. Lee TS, Lee YC. Fas/Fas ligand-mediated death pathway is involved in oxLDL-induced apoptosis in vascular smooth muscle cells. *Am J Physiol.* 2001;280:709–718.
8. Takei K, McPherson PS, Schmid SL, et al. Tubular membrane invaginations coated by dynamin rings are induced by GTP-gamma S in nerve terminals. *Nature.* 1995;374:186–190.
9. Chen MS, Ober RA, Schroeder CC, et al. Multiple forms of dynamin are encoded by Shibire, a *Drosophila* gene involved in endocytosis. *Nature.* 1991;351:583–586.

10. Nichols B. Caveosome and endocytosis of lipid rafts. *J Cell Sci*. 2003; 116:4704–4714.
11. Lakkaraju A, Rahman YE, Dubinsky JM. Low-density lipoprotein receptor–related protein mediates the endocytosis of anionic liposomes in neurons. *J Biol Chem*. 2002;277:15085–15092.
12. Yamada Y, Doi T, Hamakubo T, et al. Scavenger receptor family proteins: roles for atherosclerosis, host defense and disorders of the central nervous system. *Cell Mol Life Sci*. 1998;54:628–640.
13. Kenneth NF, Schmid LS, Damke H. Evidence that dynamin2 functions as signal-transducing GTPase. *J Cell Biol*. 2000;150:145–154.
14. Van Der Luit AH, Budde M, Verheij M, et al. Different modes of internalization of apoptotic alkyl-lysophospholipid and cell-rescuing lysophosphatidylcholine. *Biochem J*. 2003;374:747–753.
15. Roberta R, Jean-Marc Z, Angelo A. Vitamin E reduces the uptake of oxidized LDL by inhibiting CD36 scavenger receptor expression in cultured aortic smooth muscle cells. *Circulation*. 2000;102: 82–87.
16. Beverly P, Arlene M, Patricia AH, et al. Quantitative assessment of atherosclerotic lesions in mice. *Atherosclerosis*. 1987;68:231–240.
17. Kashiwakura Y, Katoh Y, Tamayose K, et al. Isolation of bone marrow stromal cell-derived smooth muscle cells by a human SM22alpha promoter: in vitro differentiation of putative smooth muscle progenitor cells of bone marrow. *Circulation*. 2003;107:2078–2081.
18. Emil A, Fusheng, Y, Greg M, et al. Multiple-label immunocytochemistry for the evaluation of nature of cell death in experimental models of neurodegeneration. *Brain Res Brain Res Protocol* 2. 2001; 7:193–202.
19. Li D, Liu L, Chen H, et al. LOX-1 mediates oxidized low-density lipoprotein-induced expression of matrix metalloproteinases in human coronary artery endothelial cells. *Circulation*. 2003;107:612–617.
20. Delettre C, Lenaers G, Pelloquin L, et al. OPA1 (Kjer type) dominant optic atrophy: a novel mitochondrial disease. *Mol Genet Metab*. 2002;75:97–107.
21. Earnest S, Khokhlatchev A, Albanesi JP, et al. Phosphorylation of dynamin br ERK2 inhibits the dynamin-microtubule interaction. *FEBS Lett*. 1996;396:62–66.
22. Gout I, Dhand R, Hiles ID, et al. The GTPase dynamin binds to and is activated by a subset of SH3 domains. *Cell*. 1993;75:25–36.
23. Lassus P, Roux P, Zugasti O, et al. Extinction of Rac1 and Cdc42Hs signaling defines a novel p53-dependent apoptotic pathway. *Oncogene*. 2000;19:2377–2385.
24. Schlunck G, Damke H, Kiosses WB, et al. Modulation of Rac localization and function by dynamin. *Mol Biol Cell*. 2004;15:256–267.

C-Reactive Protein Enhances LOX-1 Expression in Human Aortic Endothelial Cells

Relevance of LOX-1 to C-Reactive Protein–Induced Endothelial Dysfunction

Ling Li, Nadia Roumeliotis, Tatsuya Sawamura, Geneviève Renier

Abstract—C-reactive protein (CRP), a characteristic inflammatory marker, is a powerful predictor of cardiovascular events. Recent data suggest that CRP may also promote atherogenesis through inducing endothelial dysfunction. Lectin-like oxidized low-density lipoprotein (oxLDL) receptor-1 (LOX-1) is a newly identified endothelial receptor for oxLDL that plays a pivotal role in oxLDL-induced endothelial dysfunction. Whether CRP may regulate endothelial LOX-1 and induce endothelial dysfunction through this receptor is unknown. In the present study, we studied the in vitro effect of CRP on LOX-1 expression in human aortic endothelial cells (HAECs) and the role of LOX-1 in CRP-induced human monocyte adhesion to endothelium and oxLDL uptake by endothelial cells. Incubation of HAECs with CRP enhanced, in a dose- and time-dependent manner, LOX-1 mRNA and protein levels. Induction of LOX-1 protein was already present at 5 μg/mL CRP and reached a maximum at 25 μg/mL. This effect was reduced by antibodies against CD32/CD64, endothelin-1 (ET-1) and interleukin-6 (IL-6). The extent of stimulation of LOX-1 achieved by CRP was comparable to that elicited by high glucose and IL-6 and remained unchanged in presence of these factors. Finally, CRP increased, through LOX-1, both human monocyte adhesion to endothelial cells and oxLDL uptake by these cells. We conclude that CRP enhances endothelial LOX-1 expression and propose a new mechanism by which CRP may promote endothelial dysfunction, that of inducing LOX-1. (*Circ Res.* **2004;95:877-883.**)

Key Words: C-reactive protein ■ endothelium ■ lectin-like oxidized low-density lipoprotein receptor-1 ■ inflammation

Atherosclerosis is an inflammatory process that takes place in the arterial wall and is accompanied by a systemic response. Since the concept of an inflammatory soil of atherosclerosis has been validated,[1–3] serum markers of inflammation have been identified as risk markers for cardiovascular disease. Among these, highly sensitive C-reactive protein (CRP) has been proven to be the strongest predictor of cardiovascular events.[4–5] Besides being a risk marker, CRP may further play a pivotal role in promoting atherogenesis. Arguing for this hypothesis, it has been shown that CRP increases the release of inflammatory cytokines,[6] enhances the binding of monocytes to endothelium,[7] and favors macrophage foam cell formation.[8] CRP also decreases endothelial nitric oxide synthase activation while increasing the expression of endothelial cell adhesion molecules, chemokines, endothelin-1 (ET-1), and plasminogen activator inhibitor-1.[9–13]

Unregulated uptake of oxidized low-density lipoprotein (oxLDL) by vascular cells is a crucial step in atherogenesis. Endothelial lectin-like oxidized LDL receptor-1 (LOX-1) is the major receptor of oxLDL,[14] and accumulating evidences indicate that oxLDL uptake through this receptor induces endothelial dysfunction. oxLDL binding to endothelial LOX-1 generates superoxide anions, decreases nitric oxide production, and activates nuclear factor-κB (NF-κB).[15–16] Furthermore, inhibition of LOX-1 reduces oxLDL-mediated upregulation of monocyte chemoattractant protein-1 (MCP-1) and monocyte adhesion to endothelial cells.[17] Endothelial LOX-1 expression is induced by various pro-inflammatory cytokines, such as tumor necrosis factor-α (TNF-α)[18] and transforming growth factor-β (TGF-β),[19] as well as by pro-atherogenic factors, such as oxLDL and advanced glycation end products in vitro.[20] This receptor is expressed in the aortas of hypertensive,[21] diabetic,[20] and hyperlipidemic[22] animals and is upregulated in early human atherosclerotic lesions.[23] In the present study, we hypothesized that CRP-induced endothelial dysfunction may be mediated in part via LOX-1. Thus, we tested the effect of CRP on endothelial LOX-1 expression and the role of this receptor in CRP-induced monocyte adhesion and oxLDL uptake by endothelial cells.

Original received March 31, 2004; revision received August 24, 2004; accepted September 28, 2004.

From Department of Biomedical Sciences (L.L.) and Medicine (N.R., G.R.), University of Montreal, Centre Hospitalier de l'Université de Montréal (CHUM) Research Centre, Notre-Dame Hospital, Montreal, Quebec, Canada; and the Department of Bioscience (T.S.), National Cardiovascular Center Research Institute, Fujishirodai, Suita, Osaka, Japan.

Correspondence to Dr Geneviève Renier, CHUM Research Centre, Notre-Dame Hospital, J-A De Seve Pavilion, Door Y 3622, 1560 Sherbrooke St East, Montreal, Quebec H2L 4M1, Canada. E-mail genevieve.renier@umontreal.ca

Circulation Research is available at http://www.circresaha.org

DOI: 10.1161/01.RES.0000147309.54227.42

Materials and Methods

Reagents

Phenylmethylsulfonyl fluoride, Hanks balanced salt solution, penicillin–streptomycin, glycine, sodium dodecyl sulfate (SDS), and Trizol reagent were obtained from Invitrogen Life Technologies (Burlington, Ontario, Canada). Human aortic endothelial cells (HAECs), endothelial growth culture medium (EGM), and EGM bullet kit were obtained from Cedarlane Laboratories Limited (Hornby, Ontario, Canada). D-Glucose, bovine serum albumin fraction V, diamisinine dihydrochloride, hexadecyltrimethylamine ammonium bromide (HTAB), isopropanol, and E-TOXATE kit were purchased from Sigma. END-X B15 endotoxin removal affinity resin kit was obtained from Seikagaku America (Falmouth, Mass). Ficoll and horseradish peroxidase-conjugated anti-mouse IgG were obtained from Amersham Biosciences. Monoclonal antibody against β-actin was bought from Santa Cruz Biotechnology (Santa Cruz, Calif). Recombinant human interleukin-6 (IL-6), human neutralizing antibodies against IgG_1 (10 μg/mL), intercellular adhesion molecule-1 (ICAM-1) (20 μg/mL), vascular cell adhesion molecule-1 (VCAM-1) (20 μg/mL), E-selectin (20 μg/mL), IL-6 (5 μg/mL), and ET-1 (0.1 μg/mL) were purchased from R&D Systems (Minneapolis, Minn). Monoclonal antibody to human CD32 (5 μg/mL) was purchased from MEDICORP (Montreal, QC, Canada). Monoclonal antibodies to human LOX-1 (20 μg/mL) and human CD64 (5 μg/mL) were kindly provided by Dr Sawamura (National Cardiovascular Center Research Unit, Osaka, Japan) and Dr Sarfati (CHUM Research Center, Montreal, Canada), respectively. Recombinant human CRP, BAY11–7085, and actinomycin D were obtained from Calbiochem (La Jolla, Calif). 1,1′-dioctadecyl-3,3,3′,3′-tetramethylindocarbocyanine perchlorate (DiI) was bought from Molecular Probes.

Cells

Commercially available HAECs (passage 3) were grown to confluence in EGM under recommended conditions. The EGM was supplemented with 2% fetal bovine serum (FBS) containing 0.01 μg/mL human epidermal growth factor, 0.1% gentamicin sulfate amphotericin-B, 1 μg/mL hydrocortisone, and 12 μg/mL bovine brain extract protein content. Cells were used at passages 3 to 5. Confluent HAECs, cultured in medium containing 2% FBS, were exposed for different time periods to various concentrations of CRP. Endotoxin was removed from CRP using END-X B15 endotoxin removal affinity resin kit at 4°C overnight. After removal of endotoxin, CRP contained <0.03 EU/mL endotoxin, as detected by E-TOXATE kit. In some experiments, cells were pretreated with antibodies against human CD32, CD64, ET-1, or IL-6, or coincubated with CRP in the presence or absence of glucose (30 mmol/L) or IL-6.

Human monocytes were isolated as previously described.[24] Briefly, peripheral blood mononuclear cells were isolated from healthy control subjects by density centrifugation using Ficoll, allowed to aggregate in the presence of fetal calf serum, then further purified by the rosetting technique. After density centrifugation, highly purified monocytes (85% to 90%) were recovered. Human monocyte purity was assessed by flow cytometry (FACScan; Becton Dickinson) using phycoerythrin-conjugated anti-CD14 monoclonal antibody (Becton Dickinson).

Analysis of mRNA Expression

Expression of the LOX-1 gene in human HAECs cultured in 6-well plates (FALCON) was measured by polymerase chain reaction (PCR) technique. Total RNA for use in the PCR reaction was extracted from cells by an improvement of the acid–phenol technique of Chomczynski.[25] Briefly, cells were lysed with TRIzol reagent and chloroform was added to the solution. After centrifugation, the RNA present in the aqueous phase was precipitated and resuspended in diethyl pyrocarbonate water. cDNA was synthesized from RNA by incubating total cellular RNA with 0.1 μg oligodT (Pharmacia) for 5 minutes at 98°C, then by incubating the mixture with reverse transcription buffer for 1 hour at 37°C. The cDNA obtained was amplified by using 0.8 μmol/L of two synthetic primers specific for human LOX-1 (5′-TTACTCTCCATGGTGGTGCC-3′) (5′-AGCTTCTTCTDCTTGTTGCC-3′) and human glyceraldehyde-3-phosphate dehydrogenase (GAPDH) (5′-CCCTTCATTGACCT-CAACTACATGG-3′) (5′-AGTCTTCTGGGTGGCAGTGATGG-3′), used as internal standard in the PCR reaction mixture. A 193-base pair human LOX-1 cDNA fragment and a 456-base pair human GAPDH cDNA fragment were amplified enzymatically by 30 and 25 repeated cycles, respectively. An aliquot of each reaction mixture was then subjected to electrophoresis on 1% agarose gel containing ethidium bromide. The intensity of the bands was measured by an image analysis scanning system (Alpha Imager 2000; Packard Instrument Company). Titrating the cDNA samples ensured that the signal lies on the exponential part of the standard curve.

Western Blot

HAEC protein extracts (12 μg) were applied to 10% SDS-PAGE and transferred to a nitrocellulose membrane using a Bio-Rad transfer blotting system at 100 V for 1 hour. Nonspecific binding was blocked with 5% bovine serum albumin for 1 hour at room temperature. After washing with PBS–Tween 0.1%, blots were incubated overnight at 4°C with anti-LOX-1 or anti-β-actin antibodies. After further wash, membranes were incubated for 1 hour at room temperature with a horseradish peroxidase-conjugated donkey anti-mouse IgG (1/5000). Antigen detection was performed with an enhanced chemiluminescence detection system (Amersham).

Adhesion Assay

Confluent HAECs cultured in 96-well plates (FALCON) were exposed for 15 hours to 25 μg/mL CRP, then treated for 1 hour in the presence of antibodies to IgG_1 (10 μg/mL) or LOX-1. HAECs were then washed twice with Hanks balanced salt solution and incubated for 2 hours with freshly purified human monocytes (280 000 cells/well) resuspended in serum-free RPMI medium. At the end of this incubation period, nonadherent monocytes were removed by washing the cells with PBS (pH 6.0). Monocyte adhesion to HAECs was quantified by measuring monocyte myeloperoxidase (MPO) activity.[26]

Determination of Endothelial Cell-Associated Adhesion Molecule Expression

Endothelial cell surface expression of ICAM-1, VCAM-1, and E-selectin was determined by the cellular enzyme-linked immunosorbent assay method. HAECs cultured in 96-well plates (FALCON) were treated with CRP for 15 hours, and then washed with PBS. To block nonspecific binding, endothelial cells were treated for 1 hour at room temperature with PBS–3% bovine serum albumin. Twenty μg/mL of monoclonal antibodies against ICAM-1, VCAM-1, E-selectin, and control IgG_1 were then added to the cells for 2 hours at 37°C. After washing, endothelial cells were incubated for 90 minutes with horseradish-conjugated anti-mouse IgG (1/1000) (Bio-Rad). The peroxidase substrate, o-phenylnediamine dihydrochloride, was then added to the cells. The reaction was stopped by addition of 50 μL of H_2SO_4 (0.5 mol/L) and the optical density was read at 490 nm.

Uptake of DiI–oxLDL

Native LDL (density, 1.019 to 1.063) was isolated from plasma obtained from healthy donors by sequential ultracentrifugation using potassium bromide for density adjustment.[27] Native LDL was extensively dialyzed for 24 hours at 4°C against 5 mmol/L Tris/50 nmol/L NaCl to remove EDTA. Oxidation of LDL was performed by incubating native LDL (2 mg protein/mL) at 37°C for 20 hours in serum-free RPMI 1640 containing 7.5 μg/mL $CuSO_4$. Oxidation of LDL was monitored by measuring the amount of thiobarbituric acid-reactive substances (≈10 nmol malondialdehyde equivalent/mg protein) and by electrophoretic mobility on agarose gel (data not shown). Labeling of oxLDL with DiI was performed as described previously.[28] To examine cellular uptake of oxLDL, HAECs were

seated in 8-well culture slides (FALCON) and incubated for 3 hours in medium containing 5% of lipoprotein-deficient serum with DiI-labeled oxLDL (80 μg/mL) in the presence or absence of a 500-fold excess of unlabeled oxLDL. At the end of the incubation period, cells were washed, mounted on coverslips with mounting medium, and examined by fluorescence microscopy. To measure amounts of DiI-oxLDL accumulated in cells, HAECs were seated in 12-well plates receiving the same treatment as mentioned. At the end of the incubation period, DiI was extracted by isopropanol and the fluorescence was determined at 520/564 nm. Results were normalized to total cell protein concentrations.[29]

Cell Viability

Cell viability after treatment with CRP was assessed by trypan blue exclusion and determination of total cell number. It was consistently found to be higher than 95%.

Statistical Analysis

All values were expressed as the mean±SEM. Data were analyzed by one-way analysis of variance (ANOVA) followed by the Tukey test. $P<0.05$ was considered statistically significant.

Results

Effect of CRP on Endothelial LOX-1 mRNA Expression

Incubation of HAECs for 6 hours with 25 μg/mL CRP enhanced LOX-1 mRNA levels. This effect was sustained up to 24 hours (Figure 1A-a). LOX-1 mRNA levels, normalized to the levels of GAPDH mRNA (Figure 1A-b), are presented in Figure 1A-c. The stimulatory effect of CRP on LOX-1 was already present at a concentration of 5 μg/mL and was maximal with CRP concentrations ranging between 10 and 25 μg/mL (Figure 1B-a). LOX-1 mRNA levels, normalized to the levels of GAPDH mRNA (Figure 1B-b), are presented in Figure 1B-c. Preincubation of the cells with actinomycin D (5 μg/mL) for 1 hour before exposure of the cells to CRP prevented this effect (Figure 1C). Interestingly, an increase in LOX-1 mRNA expression was also observed when cells were treated for 7 days with 5 μg/mL CRP (LOX-1 gene expression [% of control values]: CRP (5 μg/mL),143±8; $P<0.05$ versus controls).

Effect of CRP on Endothelial LOX-1 Protein Expression

Treatment of HAECs for 15 hours with 25 μg/mL CRP significantly increased LOX-1 protein levels. This effect was sustained up to 48 hours (Figure 2A-a). LOX-1 protein levels normalized to the levels of β-actin (Figure 2A-b) are illustrated in Figure 2A-c. CRP-induced LOX-1 protein expression was dose-dependent, with maximal effect being observed between 10 and 25 μg/mL CRP (Figure 2B-a). LOX-1 protein levels normalized to the levels of β-actin (Figure 2B-b) are illustrated in Figure 2B-c. Because CRP binds on vascular cells to FcγRI/CD64 and FcγRIIa/CD32 receptors, we next determined whether the CRP effect on LOX-1 is receptor-mediated. HAECs were pre-incubated in the presence of antibodies to CD32 and/or CD64 before treatment with CRP. We found that CRP effect on LOX-1 was reduced, in part, by pre-incubating HAECs with anti-CD32 and anti-CD64 antibodies, and that coincubation of the endothelial cells with both antibodies totally abrogated this effect (Figure 2C). Treatment of endothelial cells with these antibodies did not influence basal LOX-1 expression (LOX-1 protein expression [% of control values]: CD32 antibody, 85±12; CD64 antibody, 102±9; CD32 +CD64 antibodies, 107±8).

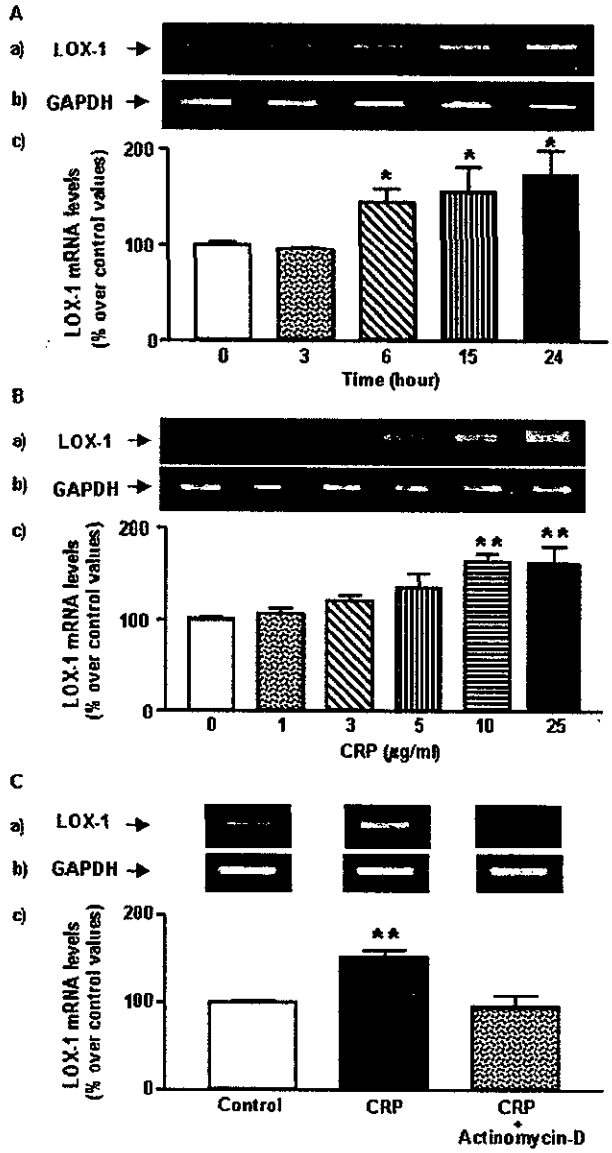

Figure 1. Time- and dose-dependent effect of CRP on LOX-1 mRNA levels in HAECs. HAECs were incubated for 3 to 24 hours with 25 μg/mL CRP (A), treated for 6 hours with 1 to 25 μg/mL CRP (B), or pre-incubated for 1 hour with 5 μg/mL actinomycin-D before being treated for 6 hours with 25 μg/mL CRP (C). At the end of the incubation period, cells were lysed and LOX-1 mRNA was analyzed by RT-PCR. LOX-1 mRNA levels (a) were normalized to the levels of GAPDH mRNA (b). Data illustrated on the graph bar (c) represent the mean±SEM of 6 different experiments. *$P<0.05$, **$P<0.01$ vs control.

Effect of IL-6 and Glucose on CRP-Induced Endothelial LOX-1 Protein Expression

Because diabetes is associated with inflammatory processes with an increase in the levels of CRP[30] and pro-inflammatory cytokines,[31,32] we studied the effect of CRP on LOX-1 expression in IL-6- and high glucose-treated HAECs. Treatment of HAECs with IL-6 (0 to 200 ng/mL) resulted in a dose-dependent increase in LOX-1 protein expression, with

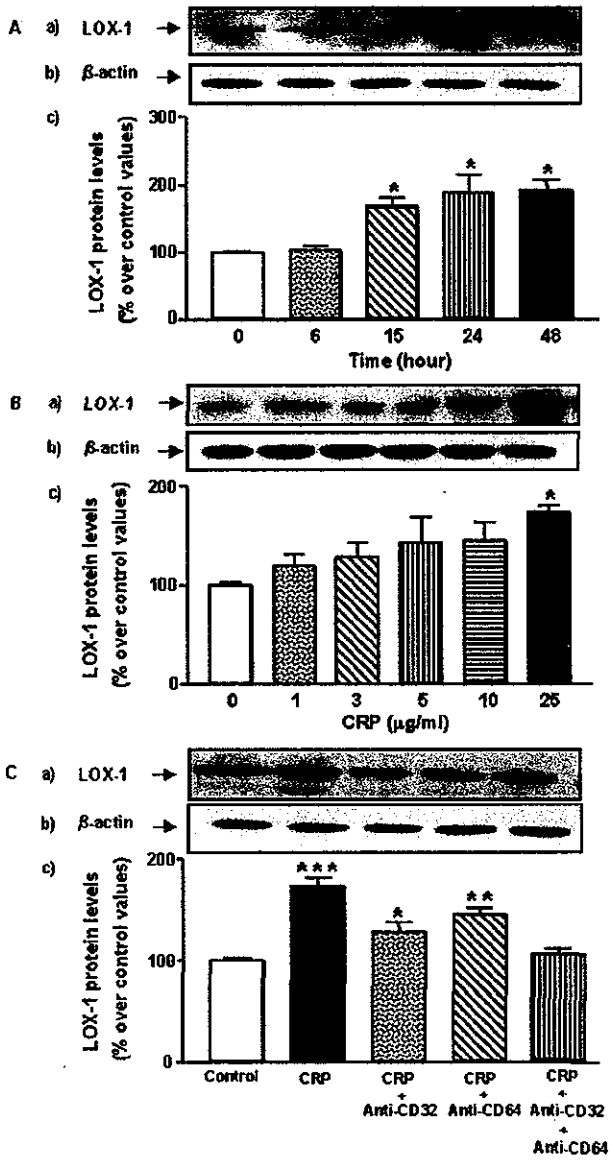

Figure 2. Time- and dose-dependent effect of CRP on endothelial LOX-1 protein expression. HAECs were cultured for 6 to 48 hours with 25 μg/mL CRP (A) or for 15 hours with 1 to 25 μg/mL CRP (B). In some experiments, HAECs were preincubated with anti-CD32 and/or anti-CD64 antibodies before treatment for 15 hours with 25 μg/mL CRP (C). At the end of the incubation period, cells were lysed and LOX-1 membrane protein expression was determined by Western blot analysis (a). LOX-1 protein levels were normalized to the levels of β-actin protein (b). Data illustrated on the graph bar represent the mean±SEM of 5 (A) and 6 (B-C) different experiments (c). *$P<0.05$, **$P<0.01$, ***$P<0.001$ vs control.

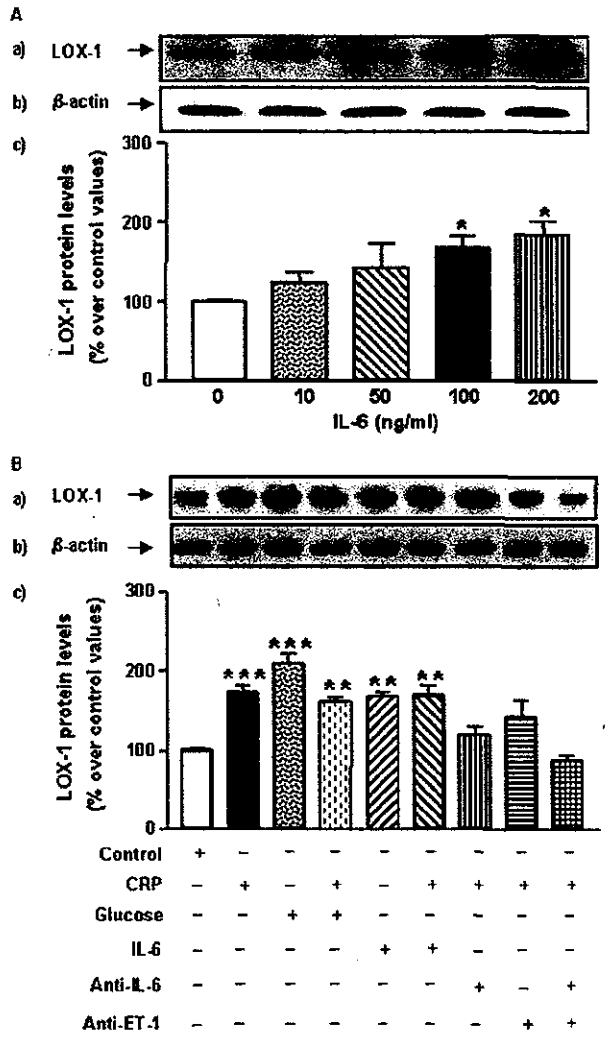

Figure 3. Effect of IL-6 and high glucose on CRP-induced endothelial LOX-1 protein expression. HAECs were incubated for 15 hours with IL-6 (10 to 200 ng/mL) (A) or treated with 25 μg/mL CRP for 15 hours in the presence or absence of glucose (30 mmol/L), IL-6 (100 ng/mL), anti-IL-6, and/or anti-ET-1 antibodies. At the end of the incubation period, cells were lysed and LOX-1 membrane protein expression was determined by Western blot analysis (a). LOX-1 protein levels were normalized to the levels of β-actin protein (b). Data illustrated on the graph bar represent the mean±SEM of 4 different experiments (c). *$P<0.05$, **$P<0.01$, ***$P<0.001$ vs control.

maximal effect at 100 to 200 ng/mL (Figure 3A). CRP did not potentiate this effect (Figure 3B). CRP-induced endothelial LOX-1 expression was reduced by ET-1 and IL-6 inhibition (Figure 3B) and coincubation of HAECs with anti-ET-1 and IL-6 antibodies totally suppressed this effect (Figure 3B). Remarkably, HAECs cultured with CRP (25 μg/mL for 15 hours) showed a 3-fold increase in IL-6 secretion (data not shown). As reported earlier,[33] incubation of HAECs in a high-glucose environment led to increased endothelial LOX-1 protein expression (Figure 3B). Addition of CRP did not further increase LOX-1 expression under hyperglycemic conditions (Figure 3B). Pretreatment of HAECs with the NF-κB inhibitor, BAY11–7085 (10 μmol/L), totally abrogated the independent and combined effects of glucose and CRP on LOX-1 expression (LOX-1 protein expression [% of control values]: glucose,193.1±13; BAY+glucose, 94±10; CRP, 160±10; BAY+CRP, 110±21; glucose+CRP, 165±11; BAY+glucose+CRP, 106±10).

CRP Enhances Monocyte Binding to HAECs: Role of LOX-1

Treatment of HAECs with CRP (25 μg/mL) or lipopolysaccharide (10 ng/mL), used in these experiments as positive control,

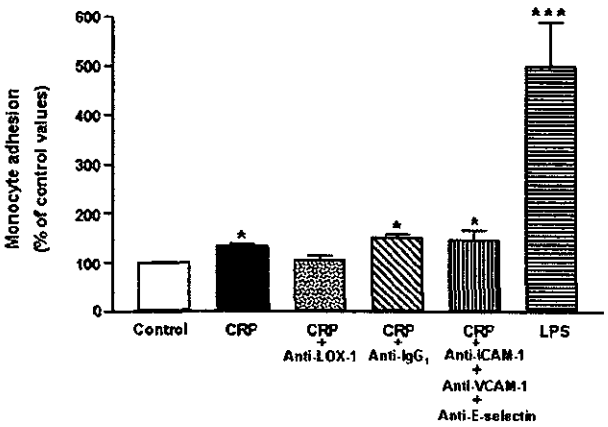

Figure 4. Effect of CRP on human monocyte adhesion to endothelial cells. Confluent HAECs were exposed for 15 hours to CRP (25 μg/mL) in the presence of saturating amounts (20 μg/mL) of antibodies to LOX-1, IgG_1, ICAM-1, VCAM-1, and E-selectin or treated for 4 hours with LPS (100 ng/mL), used as positive control. At the end of this incubation period, cells were washed and monocytes were added to HAECs to determine monocyte adhesion. Data are expressed as percentage of adherent monocytes to HAECs and represent the mean±SEM of 6 different experiments. $^*P<0.05$, $^{***}P<0.001$ vs control.

increased monocyte adhesion to these cells (Figure 4). Anti-LOX-1 antibody suppressed this effect, whereas anti-IgG_1 antibody was ineffective (Figure 4). HAECs cultured with CRP for 15 hours in medium containing 2% FBS did not show induction of ICAM-1, VCAM-1, or E-selectin expression (adhesion molecule protein expression [% over control values]: ICAM-1, 115±7; VCAM-1, 97±5; E-selectin, 90±9). Intriguingly, similar negative results were obtained when CRP was added for 6 or 24 hours to HAECs cultured in medium containing 10% or 20% FBS (data not shown). Incubation of HAECs with antibodies to ICAM-1, VCAM-1, and E-selectin failed to affect CRP-induced monocyte adhesion (Figure 4). Treatment of endothelial cells with these antibodies did not influence basal monocyte adhesion (monocyte adhesion [% of control values]: VCAM-1+ICAM-1+E-selectin antibodies, 116±11; LOX-1 antibody, 102±13).

CRP Stimulates oxLDL Uptake in Endothelial Cells Via LOX-1

To evaluate whether induction of LOX-1 by CRP results in enhanced uptake of oxLDL by endothelial cells, HAECs were treated for 14 hours with CRP (25 μg/mL), then incubation was pursued for 1 hour in the presence of saturating amounts (20 μg/mL) of antibodies to LOX-1 or IgG_1. At the end of the incubation period, cells were exposed for 3 hours to DiI–oxLDL (80 μg/mL) in the presence or absence of excess unlabeled oxLDL. Incubation of HAECs with CRP led to enhanced uptake of oxLDL by these cells as assessed by fluorescence microscopy (Figure 5A) and measurement of extracted DiI–oxLDL (Figure 5B). This effect was abrogated by incubating HAECs with anti-LOX-1 antibody or with excess unlabeled oxLDL. In contrast, exposure of these cells to anti-IgG_1 did not affect CRP-induced oxLDL uptake by endothelial cells (Figure 5A and 5B).

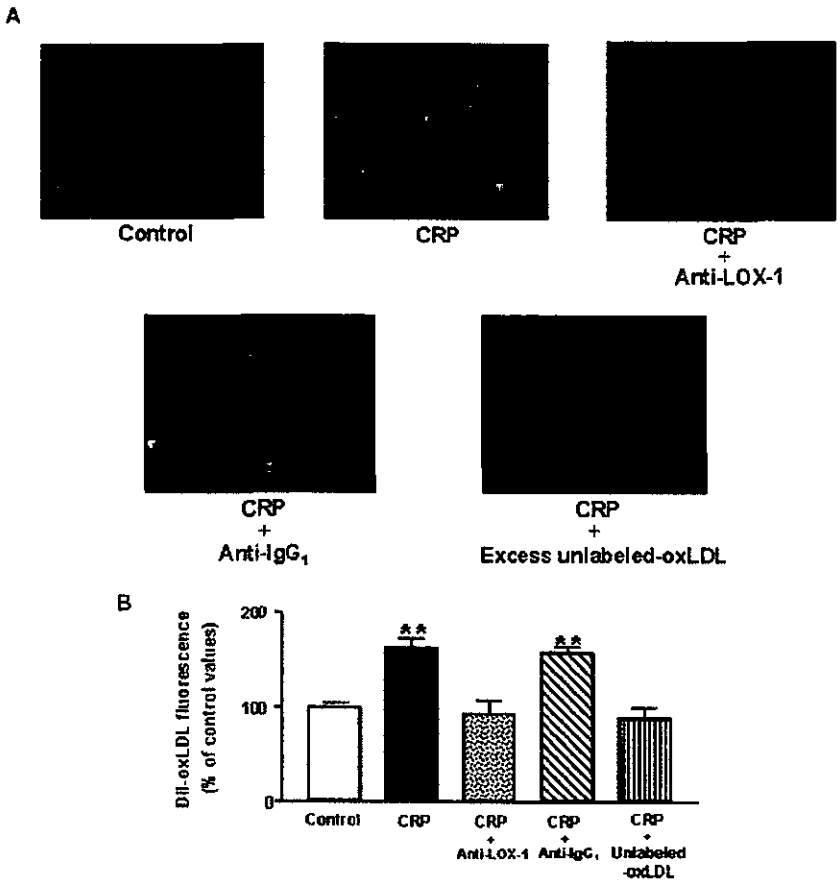

Figure 5. Effect of CRP on oxLDL uptake by HAECs. HAECs were treated for 14 hours with CRP (25 μg/mL), and then incubation was pursued for an additional 1 hour period in the presence of saturating amounts (20 μg/mL) of antibodies to LOX-1 or IgG_1. At the end of the incubation period, cells were exposed for 3 hours to DiI–oxLDL (80 μg/mL) in the presence or absence of excess unlabeled oxLDL. After washing, fluorescence of DiI was detected in cytoplasm of HAECs by fluorescence microscopy (A) or measured at 520/564 nm (B). Data illustrated on the graph bar represent the mean±SEM of 6 independent experiments. $^{**}P<0.01$ vs control.

Discussion

Accumulating evidences indicate that chronic low-grade inflammation is a major pathogenic component of endothelial dysfunction.[1] Consistent with this concept, elevated serum CRP levels have been found to be associated with blunted endothelium-dependent vasodilation in vivo,[34] and a direct proinflammatory effect of CRP on endothelial cells has been documented in vitro.[9–13] The present study, which demonstrates that CRP enhances the expression of LOX-1, a limiting factor for oxLDL uptake by endothelial cells, further stresses the potential key role of CRP in endothelial dysfunction. Induction of LOX-1 by CRP is receptor-mediated and appears to be exerted at the transcriptional level, as reflected by the parallel increase in LOX-1 gene and protein expression and the inhibitory effect of actinomycin D on CRP-induced LOX-1 gene expression. Transcriptional activation of the LOX-1 gene by CRP may theoretically involve NF-κB. Supporting this possibility, a NF-κB–responsive element has been located in the promoter of the LOX-1 gene,[35] and increased transcriptional activity of this factor has been documented in CRP-treated endothelial cells.[36] CRP predicts incident type 2 diabetes[37,38] and is increased in subjects with diabetes.[30] Thus, hyperglycemia, in states of high CRP, may exaggerate the deleterious effects of CRP on endothelial cell activation. In contrast to previous observations showing that high glucose potentiates the proatherogenic effects of CRP in endothelial cells,[13,39] we found that induction of LOX-1 by CRP remained unchanged by hyperglycemia, suggesting that CRP and glucose may operate through common molecular mechanisms to induce LOX-1. Because glucose induces endothelial LOX-1 through NF-κB activation,[33] and because CRP activates this transcription factor in endothelial cells,[36] NF-κB may represent a common signal mediator of CRP and glucose effect on LOX-1. Our data, which show that inhibition of NF-κB prevents LOX-1 induction elicited by these two agents, support this possibility.

CRP and glucose are well-known activators of ET-1 release by endothelial cells,[11,40] and this peptide mediates the proinflammatory effects of CRP.[11] Interestingly, ET-1 is also a LOX-1 stimulatory factor,[41] and thus may mediate CRP effect on LOX-1. In support of this possibility, our data demonstrate that inhibition of ET-1 attenuates CRP effect on LOX-1. ET-1 is one of the upstream activators of IL-6 secretion,[42] and recent data suggest that CRP may stimulate the release of this cytokine by endothelial cells.[11] Our observation that CRP exerts a direct stimulatory effect on IL-6 secretion by cultured HAECs, and our findings that IL-6 induces endothelial LOX-1 and that inhibition of IL-6 reduces CRP-induced LOX-1 expression strongly support a role of IL-6 as one mediator of CRP effect on LOX-1. Our finding that attenuation of CRP-induced LOX-1 expression was greater during coincubation with anti-ET-1 and IL-6 antibodies support the concept that CRP induces LOX-1 via stimulating the production of ET-1 and IL-6 concurrently.

One major pathophysiological event associated with endothelial dysfunction is increased monocyte adhesion to endothelial cells. Recent studies have demonstrated that CRP increases monocyte–endothelium interaction[7,43] by inducing endothelial and monocyte adhesion molecules.[7–9,11,44,45] Our findings that CRP increases the expression of LOX-1, a well-identified cell adhesion molecule,[46] and that blockade of LOX-1 abolished CRP-induced monocyte adhesion, suggest a new role for LOX-1, that of mediating the stimulatory effect of CRP on monocyte adhesion. The similar 1.5-fold increase in adhesion of mononuclear leukocytes documented in CRP-treated endothelial cells and CHO-K1 cells expressing human LOX-1[47] further stress this possibility.

In contrast to previous studies showing that CRP increases the expression of E-selectin, ICAM-1, and VCAM-1 in endothelial cells,[8,11,44,45] we did not observe an upregulation of these antigens in CRP-treated HAECs, regardless of the concentrations of serum present in the culture medium or the time incubation periods with CRP. These results differ from previous findings that CRP-induced expression of adhesion molecules is serum- and time-dependent.[8,45] Although the reasons for these discrepancies remain unknown, some experimental conditions specifically used in our work, such as the use of heat-inactivated serum, very low-endotoxin CRP, and cell enzyme-linked immunosorbent assay for adhesion molecule detection, might provide an explanation for these apparent conflicting results.

Endothelial cells do express different types of modified LDL scavenger receptors, including SR-A, SR-B, CD36, SREC, and LOX-1. Although it has long been suggested that endothelial cells internalize and degrade modified LDL, previous studies have suggested that this process occurs through a receptor-mediated pathway that does not involve classic scavenger receptors.[48] These data and the recent finding that endothelial cells internalize and degrade oxLDL via the LOX-1 receptor[14] support the notion that LOX-1 is the major receptor for oxLDL expressed in endothelial cells, presumably mediating the majority of the uptake of oxLDL by these cells. Our results showing that CRP enhances, through LOX-1, the uptake of oxLDL by endothelial cells suggest that CRP may trigger the toxic effect of oxLDL on vascular endothelium.

In conclusion, the present study demonstrates that CRP, at concentrations applicable to both acute and low-grade chronic inflammation, increases endothelial LOX-1 expression. Whether this potentially pro-atherogenic effect of CRP has clinical relevance remains to be evaluated.

Acknowledgments

This study was supported by a grant from the Association Diabète Québec.

References

1. Ross R. Atherosclerosis is an inflammatory disease. *Am Heart J*. 1999; 138:S419–S420.
2. Libby P. Inflammation in atherosclerosis. *Nature*. 2002;420:868–874.
3. Fan J, Watanabe T. Inflammatory reactions in the pathogenesis of atherosclerosis. *J Atheroscler Thromb*. 2003;10:63–71.
4. Shah SH, Newby LK. C-reactive protein: a novel marker of cardiovascular risk. *Cardiol Rev*. 2003;11:169–179.
5. Ridker PM, Hennekens CH, Buring JE, Rifai N. C-reactive protein and other markers of inflammation in the prediction of cardiovascular disease in women. *N Engl J Med*. 2000;342:836–843.
6. Ballou SP, Lozanski G. Induction of inflammatory cytokine release from cultured human monocytes by C-reactive protein. *Cytokine*. 1992;4: 361–368.
7. Woollard KJ, Phillips DC, Griffiths HR. Direct modulatory effect of C-reactive protein on primary human monocyte adhesion to human endothelial cells. *Clin Exp Immunol*. 2002;130:256–262.
8. Fu T, Borensztajn J. Macrophage uptake of low-density lipoprotein bound to aggregated C-reactive protein: possible mechanism of foam-cell formation in atherosclerotic lesions. *Biochem J*. 2002;366:195–201.

9. Pasceri V, Willerson JT, Yeh ET. Direct proinflammatory effect of C-reactive protein on human endothelial cells. *Circulation*. 2000;102: 2165–2168.
10. Pasceri V, Cheng JS, Willerson JT, Yeh ET, Chang J. Modulation of C-reactive protein-mediated monocyte chemoattractant protein-1 induction in human endothelial cells by anti-atherosclerosis drugs. *Circulation*. 2001;103:2531–2534.
11. Verma S, Li SH, Badiwala MV, Weisel RD, Fedak PW, Li RK, Dhillon B, Mickle DA. Endothelin antagonism and interleukin-6 inhibition attenuate the proatherogenic effects of C-reactive protein. *Circulation*. 2002;105:1890–1896.
12. Verma S, Wang CH, Li SH, Dumont AS, Fedak PW, Badiwala MV, Dhillon B, Weisel RD, Li RK, Mickle DA, Stewart DJ. A self-fulfilling prophecy: C-reactive protein attenuates nitric oxide production and inhibits angiogenesis. *Circulation*. 2002;106:913–919.
13. Devaraj S, Xu DY, Jialal I. C-reactive protein increases plasminogen activator inhibitor-1 expression and activity in human aortic endothelial cells: implications for the metabolic syndrome and atherothrombosis. *Circulation*. 2003;107:398–404.
14. Sawamura T, Kume N, Aoyama T, Moriwaki H, Hoshikawa H, Aiba Y, Tanaka T, Miwa S, Katsura Y, Kita T, Masaki T. An endothelial receptor for oxidized low-density lipoprotein. *Nature*. 1997;386:73–74.
15. Cominacini L, Pasini AF, Garbin U, Davoli A, Tosetti ML, Campagnola M, Rigoni A, Pastorino AM, Lo Cascio V, Sawamura T. Oxidized low density lipoprotein (ox-LDL) binding to ox-LDL receptor-1 in endothelial cells induces the activation of NF-κB through an increased production of intracellular reactive oxygen species. *J Biol Chem*. 2000;275: 12633–12638.
16. Cominacini L, Rigoni A, Pasini AF, Garbin U, Davoli A, Campagnola M, Pastorino AM, Lo Cascio U, Sawamura T. The binding of oxidized low-density lipoprotein (oxLDL) to ox-LDL receptor-a in endothelial cells reduces the intracellular concentration of nitric oxide through an increased production of superoxide. *J Biol Chem*. 2001;276:13750–13755.
17. Li D, Mehta J. L. Antisense to LOX-1 inhibits oxidized LDL-mediated upregulation of monocyte chemoattractant protein-1 and monocyte adhesion to human coronary artery endothelial cells. *Circulation*. 2000; 101:2889–2895.
18. Kume N, Murase T, Moriwaki H, Aoyama T, Sawamura T, Masaki T, Kita T. Inducible expression of lectin-like oxidized LDL receptor-1 in vascular endothelial cells. *Circ Res*. 1998;83:322–327.
19. Draude G, Lorenz R. L. TGF-β 1 downregulates CD36 and scavenger receptor A but upregulates LOX-1 in human macrophages. *Am J Physiol Heart Circ Physiol*. 2000;278:H1042–H1048.
20. Chen M, Nagase M, Fujita T, Narumiya S, Masaki T, Sawamura T. Diabetes enhances lectin-like oxidized LDL receptor-1 (LOX-1) expression in the vascular endothelium: possible role of LOX-1 ligand and AGE. *Biochem Biophys Res Commun*. 2001;287:962–968.
21. Nagase M, Hirose S, Sawamura T, Masaki T, Fujita T. Enhanced expression of endothelial oxidized low-density lipoprotein receptor (LOX-1) in hypertensive rats. *Biochem Biophys Res Commun*. 1997;237: 496–498.
22. Chen M, Kakutani M, Minami M, Kataoka H, Kume N, Narumiya S, Kita T, Sawamura T. Increased expression of lectin-like oxidized low density lipoprotein receptor-1 in initial atherosclerotic lesions of Watanabe heritable hyperlipidemic rabbits. *Arterioscler Thromb Vasc Biol*. 2000;20: 1107–1115.
23. Kataoka H, Kume N, Miyamoto S, Minami M, Moriwaki H, Murase T, Sawamura T, Masaki T, Hashimoto N, Kita T. Expression of lectin-like oxidized low-density lipoprotein receptor-1 in human atherosclerotic lesions. *Circulation*. 1999;99:3110–3117.
24. Mentzer SJ, Guyre PM, Burakoff SJ, Faller DV. Spontaneous aggregation as a mechanism for human monocyte purification. *Cell Immunol*. 1986: 101:312–319.
25. Chomczynski P, Sacchi N. Single step method of RNA isolation by acid guanidinium thiocyanate-phenol-chloroform extraction. *Anal Biochem*. 1987;162:56–159.
26. Wang J, Beekhuizen H, van Furth R. Surface molecules involved in the adherence of recombinant interferon-gamma (rIFN-gamma)-stimulated human monocytes to vascular endothelium cells. *Clin Exp Immunol*. 1994;95:263–269.
27. Hatch FT. Practical methods for plasma lipoprotein analysis. *Adv Lipid Res*. 1968;6:1–68.
28. Stephan ZF, Yurachek EC. Rapid fluorometric assay of LDL receptor activity by Dil-labeled LDL. *J Lipid Res*. 1993;34:325–330.
29. Bradford MM. A rapid and sensitive method for the quantification of microgram quantities of protein utilizing the principle of protein-dye binding. *Anal Biochem*. 1976;72:248–254.
30. Rodriguez-Moran M, Guerrero-Romero F. Increased levels of C-reactive protein in noncontrolled type II diabetic subjects. *J Diabetes Complications*. 1999;13:211–215.
31. Theuma P, Fonseca VA. Inflammation and emerging risk factors in diabetes mellitus and atherosclerosis. *Curr Diab Rep*. 2003;3:248–254.
32. Dandona P. Endothelium, inflammation, and diabetes. *Curr Diab Rep*. 2002;2:311–315.
33. Li L, Sawamura T, Renier G. Glucose enhances endothelial LOX-1 expression: role for LOX-1 in glucose-induced human monocyte adhesion to endothelium. *Diabetes*. 2003;52:1843–1850.
34. Fichtlscherer S, Rosenberger G, Walter DH, Breuer S, Dimmeler S, Zeiher AM. Elevated C-reactive protein levels and impaired endothelial vasoreactivity in patients with coronary artery disease. *Circulation*. 2000: 102:1000–1006.
35. Nagase M, Abe J, Takahashi K, Ando J, Hirose S, Fujita T. Genomic organization and regulation of expression of the lectin-like oxidized low-density lipoprotein receptor (LOX-1) gene. *J Biol Chem*. 1998;273: 33702–33707.
36. Verma S, Badiwala MV, Weisel RD, Li SH, Wang CH, Fedak PW, Li RK, Mickle DA. C-reactive protein activates the nuclear factor-kappaB signal transduction pathway in saphenous vein endothelial cells: implications for atherosclerosis and restenosis. *J Thorac Cardiovasc Surg*. 2003;126:1886–1891.
37. Pradhan AD, Manson JE, Rifai N, Buring JE, Ridker PM. C-reactive protein, interleukin 6, and the risk of developing type II diabetes mellitus. *JAMA*. 2001;286:327–334.
38. Freeman DJ, Norrie J, Caslake MJ Gaw A, Ford L, Lowe GD, O'Reilly DS, Packard CJ, Sattar N, West of Scotland Coronary Prevention Study C-reactive protein is an independent predictor of risk for the development of diabetes in the West of Scotland Coronary Prevention Study. *Diabetes*. 2002;51:1596–1600.
39. Verma S, Wang CH, Weisel RD, Badiwala MV, Li SH, Fedak PW, Li RK, Mickle DA. Hyperglycemia potentiates the proatherogenic effects of C-reactive protein: reversal with rosiglitazone. *J Mol Cell Cardiol*. 2003; 35:417–419.
40. Park JY, Takahara N, Gabriele A Chou E, Naruse K, Suzuma K, Yamauchi T, Ha SW, Meier M, Rhodes CJ, King GL. Induction of endothelin-1 expression by glucose: an effect of protein kinase C activation. *Diabetes*. 2000;49:1239–1248.
41. Morawietz H, Duerrschmidt N, Niemann B Galle J, Sawamura T, Holtz J. Induction of the oxLDL receptor LOX-1 by endothelin-1 in human endothelial cells. *Biochem Biophys Res Commun*. 2001;284:961–965.
42. Browatzki M, Schmidt J, Kubler W Kranzhofer R. Endothelin-1 induces interleukin-6 release via activation of the transcription factor NF-κB in human vascular smooth muscle cells. *Basic Res Cardiol*. 2000;95: 98–105.
43. Torzewski M, Rist C, Mortensen RF, Zwaka TP, Bienek M, Waltenberger J, Koening W, Schmitz G, Hombach V, Torzewski J. C-reactive protein in the arterial intima: role of C-reactive protein receptor-dependent monocyte recruitment in atherosclerosis. *Arterioscler Thromb Vasc Biol*. 2000;20:2094–2099.
44. Blann AD, Lip GY. Effects of C-reactive protein on the release of von Willebrand factor, E-selectin, thrombomodulin and intercellular adhesion molecule-1 from human umbilical vein endothelial cells. *Blood Coagul Fibrinolysis*. 2003;14:335–340.
45. Wadham C, Albanese N, Roberts J, Wang L, Bagley CJ, Gamble JR, Rye K-A, Barter PJ, Vadas MA, Xia P. High-density lipoproteins neutralize C-reactive protein proinflammatory activity. *Circulation*. 2004;109: 2115–2121.
46. Honjo M, Nakamura K, Yamashiro K, Kiryu J, Tanihara H, McEvoy LM, Honda Y, Butcher EC, Masaki T, Sawamura T. Lectin-like oxidized LDL receptor-1 is a cell-adhesion molecule involved in endotoxin-induced inflammation. *Proc Natl Acad Sci U S A*. 2003;100:1274–1279.
47. Hayashida K, Kume N, Minami M, Kita T. Lectin-like oxidized LDL receptor-1 (LOX-1) supports adhesion of mononuclear leukocytes and a monocyte-like cell line THP-1 cells under static and flow conditions. *FEBS Letters*. 2002;511:133–138.
48. Kume N, Arai H, Kawai C, Kita T. Receptors for modified low-density lipoproteins on human endothelial cells: different recognition for acetylated low-density lipoprotein and oxidized low-density lipoprotein. *Biochim Biophys Acta*. 1991;1091:63–67.

Induction of Endothelin-1 Production in Endothelial Cells Via Co-Operative Action Between CD40 and Lectin-like Oxidized LDL Receptor (LOX-1)

Kanako Sakurai†, Luciano Cominacini‡, Ulisse Garbin‡, Anna Fratta Pasini‡, Noriko Sasaki†, Yoh Takuwa*, Tomoh Masaki†, and Tatsuya Sawamura†***

Abstract: Lectin-like oxidized low-density lipoprotein receptor-1 (LOX-1), originally identified as the major receptor for oxidized low-density lipoprotein in endothelial cells, mediates the interaction between activated platelets and endothelial cells. Stimulation of LOX-1 causes various functional changes in endothelial cells relevant to 'endothelial dysfunction'. This study investigated the cellular responses to platelet binding via LOX-1, comparing it with CD40, which also mediates platelet-binding in endothelial cells. Activated platelets, which bind both LOX-1 and CD40, induced endothelin-1 production via co-operation of LOX-1 and CD40. Stimulation of LOX-1 by oxidized low-density lipoprotein induced the expression of CD40 as well as LOX-1 itself, and stimulation of CD40 by CD40L induced the expression of LOX-1 as well as CD40. Activated platelets induced both LOX-1 and CD40 expression via these two systems in endothelial cells. Application of superoxide dismutase suppressed LOX-1-mediated, but not CD40-mediated, induction of endothelin-1. LOX-1 and CD40 synergistically, but through a distinct pathway, work to induce endothelin-1 expression in endothelial cells. This co-operative action between LOX-1 and CD40 might play a key role in the induction of endothelial dysfunction.

Key Words: endothelin-1, CD40, platelet, endothelium, oxidized LDL, lectin-like oxidized LDL receptor-1

(*J Cardiovasc Pharmacol*™ 2004;44(suppl 1):S173–S180)

Oxidatively modified low-density lipoprotein (OxLDL) is thought to be one of the major causes of endothelial dysfunction associated with proatherogenic conditions.[1] It induces in endothelial cells the expression of adhesion molecules (e.g. intercellular adhesion molecule-1, vascular cell adhesion molecule-1) and E-selectin; it stimulates the release of chemokines and smooth muscle growth factors; and it impairs endothelium-dependent vasorelaxation. This results in the recruitment of leukocytes into the sub-endothelial space, proliferation of smooth muscle cells,[2] and an increase in vascular tonus. These functional changes of endothelial cells are recognized as 'endothelial dysfunction', which is purported to be an initial step to vascular malfunction and morphological changes. Lectin-like oxidized low-density lipoprotein receptor-1 (LOX-1)[3] has been successfully identified and reported as the molecule that mediates the effects of OxLDL on endothelial cells. Expression of LOX-1 in endothelial cells is relatively low in basal conditions, but it can be induced by proinflammatory cytokines and vasoconstrictive peptides in vitro.[4] In vivo, LOX-1 expression is enhanced in proatherogenic settings including hypertension, diabetes, and hyperlipidemia, and is accumulated in the atherosclerotic lesion.[5–9] In endothelial cells, activation of LOX-1 by OxLDL induces upregulation of monocyte chemotactic protein-1, intercellular adhesion molecule-1, and vascular cell adhesion molecule-1 expression,[10,11] and a reduction in the release of nitric oxide,[12] which are characteristics of 'endothelial dysfunction'. The binding of platelets to LOX-1 enhances the release of endothelin-1 (ET-1) and suppresses the release of nitric oxide from endothelial cells.[13,14] This suggests that platelet-endothelium interaction via LOX-1 might induce endothelial changes in a similar way to OxLDL. The CD40–CD40 ligand (CD40L) system has been shown to play an essential role in several immunogenic and inflammatory processes. The CD40L and CD40 are members of the tumor necrosis factor-α and tumor necrosis factor receptor families, respectively. The expression of CD40 in endothelial cells[15] and CD40L in platelets[16] other than T-cells has been reported. Stimulation of CD40 in endothelial cells induces the expression of adhesion molecules, proinflammatory cytokines, and chemokines.[15,16] Thus LOX-1 and CD40 might play a pivotal role in endothelial dysfunction, especially in platelet–endothelium interaction. The function of the two systems appears to be overlapping. In this study, we examined the communication of these two functionally

*Department of Physiology, Kanazawa University Graduate School of Medicine, Kanazawa, Japan; †Department of Vascular Physiology, National Cardiovascular Center Research Institute, Suita, Japan; ‡Department of Biomedical and Surgical Sciences (Medicina D), University of Verona, Verona, Italy; **Department of Molecular Pathophysiology, Osaka University Graduate School of Pharmaceutical Sciences, Suita, Japan

Address correspondence and reprint requests to Dr Tatsuya Sawamura, Department of Vascular Physiology, National Cardiovascular Center Research Institute, Suita, 565-8565 Osaka, Japan. E-mail: t-sawamura@umin.ac.jp

related systems in mediating endothelial dysfunction, analyzing their expression and ET-1 production.

METHODS

Preparation of Oxidized LDL

Human LDL ($d = 1.019–1.063$) was isolated, as previously described,[3] from fresh plasma of a healthy human by sequential ultracentrifugation at 4°C. Oxidative modification of LDL was performed by incubation with 7.5 μmol/L $CuSO_4$ at 37°C for 12 hours. Oxidation was monitored by measuring the amount of thiobarbituric acid-reactive substances. The resultant OxLDL contained approximately 10 nmol/L of malondialdehyde equivalent/mg of protein. The relative electrophoretic mobility of the OxLDL to native LDL was about 2.10.

Cloning and Generation of Stable Cell Line Expressing Human CD40 and CD40L

Total RNA was purified with TRIZOL reagent (Invitrogen, Carlsbad, CA, USA) from human mononuclear cells isolated from whole blood using Ficoll-Paque (Amersham Pharmacia Biotech, Little Chalfont, Buckinghamshire, U.K.). Then 5 μg of total RNA were reverse transcribed with 200 units of superscript II (Invitrogen) and oligo(dT) primer. To amplify the coding region of human CD40 and CD40L, 5 μL of the reaction were amplified with LA-Taq DNA-polymerase (Takara, Otsu, Japan) using the following primer pairs: human CD40 (sense primer, 5′-TCGCCATGGTTCGTCTGCCTCTGC-3′; antisense primer, 5′-CTGTCTCTCCTGCACTGAGATGCG-3′); human CD40L (sense primer, 5′-CACAGCATGATCGAAACA-TACA-3′; antisense primer, 5′-GAGTTTGAGTAAGCC-AAAGGA-3′).

The cDNA fragments of CD40 and CD40L amplified by these primers, deleting the original stop codon, were subcloned into pCDNA3.1/V5-His-TOPO vector (CD40; Invitrogen) or pEF6/V5-His-TOPO vector (CD40L; Invitrogen), to be in-frame fusions of the V5 epitope at the C-terminus. The sequences of the subcloned CD40 and CD40L cDNAs were confirmed by a sequencer (ABI model 310; Applied Biosystems, Foster City, CA, U.S.A.) with an ABI Dye Terminator kit.

In order to generate stable cell lines expressing human CD40 (hCD40-CHO-K1) or human CD40L (hCD40L-CHO-K1), pCDNA3.1 human CD40-V5 and pPUR (Clontech, Palo Alto, CA, U.S.A.), or pEF6 human CD40L-V5 and pPUR were co-transfected into CHO-K1 cells by using lipofectamine 2000 (Invitrogen). Stable cell lines were selected with 10 μg/mL of puromycin.

Preparation of Platelets

Washed platelets were prepared from blood from healthy volunteers as described previously.[13] In order to obtain activated platelets, the suspension of washed platelets was stimulated with 1 unit/mL of thrombin and 20 μg/mL of collagen for 20 minutes at 37°C. Then, 1 unit/mL of hirudin (Calbiochem, San Diego, CA, U.S.A.) was added to stop the reaction of thrombin. The density of the platelets was adjusted to 1×10^7/mL in Hepes-Tyrode's buffer.

Platelet Binding Assay

Platelets were labeled with fluorescent calcein by incubating with 1 μmol/L calcein-acetoxymethyl ester (Molecular Probes, Eugene, OR, U.S.A.) for 30 minutes at 37°C, as described.[13] After labeling, platelets were washed twice with Hepes-Tyrode's buffer and subjected to incubation with cells for 1 hour at 4°C at the density of 1×10^7/mL. The cells were washed with Hepes-Tyrode's buffer twice to remove unbound platelets, and were lysed with 0.1% sodium dodecyl sulfate/Hepes-Tyrode's buffer. The fluorescence of calcein in the cell lysate was determined by a spectrofluorometer (excitation 488 nm; emission 515–545 nm; Spectro Fluor, Tecan, Maennedorf, Switzerland), to quantify the binding of platelets.

Stimulation of BAEC by Oxidized LDL, CD40L, and Platelets

Quiescent, confluent bovine aortic endothelial cells (BAEC) were incubated with 30 μg/mL of OxLDL, 1×10^5/mL of hCD40L-CHO-K1, or 1×10^7/mL of platelets at 37°C for 8 hours. Then the culture medium was collected for the determination of ET-1 concentration, and cells were collected for reverse transcriptase-polymerase chain reaction (RT-PCR) or Western blotting. In some experiments, blocking antibodies (or control mouse immunoglobulin G) to bovine LOX-1 (JTX-20, 10 μg/mL), with either human CD40L (TRAP1, 10 μg/mL; Immunotec, Marseille, France) or superoxide dismutase (SOD, 50U), were added to the culture medium 30 minutes before stimulation.

RT-PCR

cDNA was prepared from 1 μg of total RNA from BAEC and was subjected to polymerase chain reaction (PCR) testing, as above, by the use of specific primer pairs: bovine LOX-1 (sense primer, 5′-GAAGGCGAATCTATT GAGAGC-3′; antisense primer, 5′-CTTCTCTGAAGTCC TGCAGG-3′); bovine CD40 (sense primer, 5′-TGTCACGAGCACAGATACTGC-3′; antisense primer, 5′-GACACGTTGGAGAAGAAGCC-3′); and bovine ET-1 (sense primer, 5′-TACAACCGTGCTCACTGAGG-3′; antisense primer, 5′-ATGGAGACAAGACTGGCTGG-3′). The thermal cycler settings were: for bovine LOX-1 30 cycles of 40 seconds at 94°C, 1 minute at 55°C and 1 minute at 72°C; for bovine CD40 30 cycles of 40 seconds at 94°C, 1 minute at 57°C and 1 minute at 72°C; and for ET-1 30 cycles of 40 seconds at 94°C, 1 minute at 58°C and 1 minute

at 72°C. cDNA for bovine glyceraldehyde-3-phosphate dehydrogenase (GAPDH) was amplified as an internal control (sense primer, 5′-GACCACAGTCCATGACAT-CACT-3′; antisense primer, 5′-TCCACCACCCTGTTG-CTGTAG-3′). The thermal cycler setting was 25 cycles of 40 seconds at 94°C, 1 minute at 60°C and 1 minute at 72°C.

Amplified transcripts were separated in 4% agarose gel and visualized with ethidium bromide under ultraviolet radiation. The amplification products were of expected size [bovine LOX-1 269 base pairs (bp), bovine CD40 236 bp, bovine ET-1 225 bp, and bovine GAPDH 453 bp]. The signal intensity of each amplified product was quantified and normalized according to that of GAPDH.

Western Blot Analysis

The membrane fractions of the cells obtained as pellets of ultracentrifugation at 100 000 *g* for 1 hour were separated by sodium dodecyl sulfate/polyacrylamide gel electrophoresis and transferred on to polyvinylidene difluoride membranes (Immobilon-P SQ; Millipore, Bedford, MA, U.S.A.). The membranes were probed with anti-LOX-1 monoclonal antibody (No. 5-2) and anti-CD40 polyclonal antibody (H-120; Santa Cruz Biotechnology, Santa Cruz, CA, U.S.A.).

Measurement of ET-1 Production from BAEC

Concentrations of ET-1 in culture media were determined using a sandwich enzyme immunoassay kit (IBL, Gunma, Japan) as described.[13]

Statistics

Results are expressed as the means ± standard error of the mean (SEM). Statistical analyses were performed using analysis of variance and Student's *t*-test. A *P*-value < 0.05 was considered to be statistically significant.

RESULTS

LOX-1 and CD40 Mediate Platelet-binding to Endothelial Cells

The binding of platelets fluorescently labeled with calcein to bLOX-1-CHO-K1 and hCD40-CHO-K1 were examined. Quantitative analyses of binding by spectrofluorometer revealed that bLOX-1-CHO-K1 and hCD40-CHO-K1 significantly bind thrombin-activated platelets, while resting platelets did not show binding to either LOX-1 or CD40. The results suggest that platelet bindings mediated by both LOX-1 and CD40 were activation-dependent (Fig. 1A, B). The binding of platelets to bLOX-1-CHO-K1 and hCD40-CHO-K1 were inhibited by blocking antibodies, anti-LOX-1 and anti-CD40L, respectively, confirming that these bindings were actually mediated by LOX-1 and CD40. In contrast, CHO-K1 cells did not show any significant binding of activated platelets. The binding of platelets to BAEC was also activation-dependent and inhibited by anti-

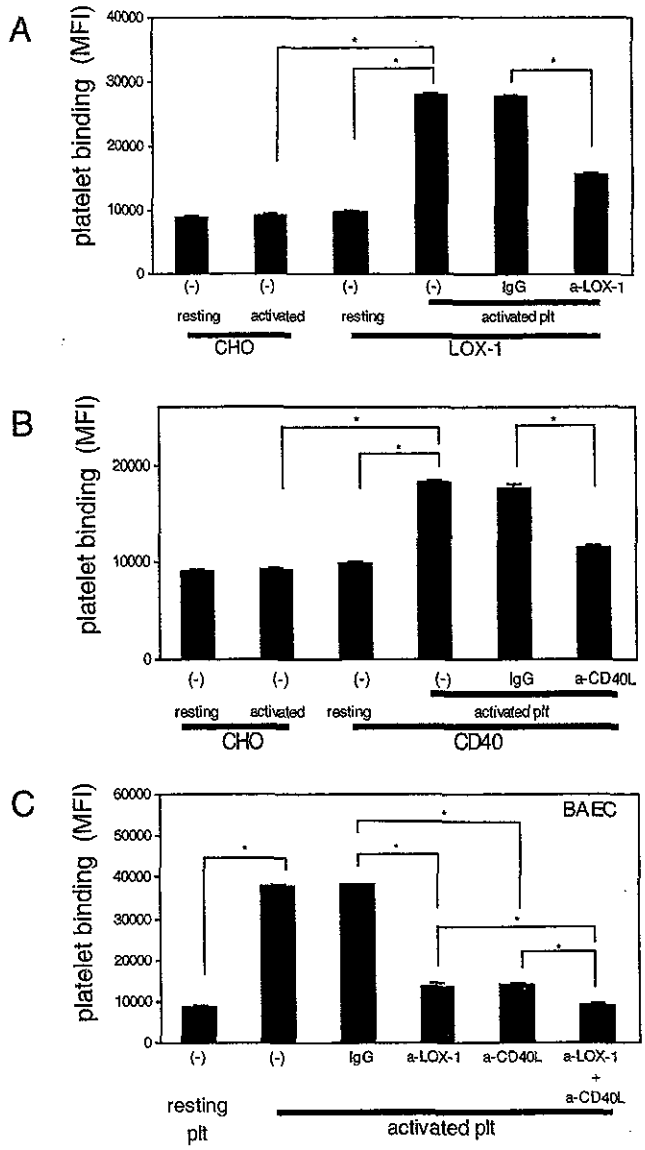

FIGURE 1. The binding of platelets (plt) mediated by lectin-like oxidized low-density lipoprotein receptor-1 (LOX-1) and CD40. Fluorescently labeled platelets (1×10^7/mL) were incubated with (A) LOX-1-expressing cells, (B) CD40-expressing cells or (C) bovine aortic endothelial cells (BAEC) for 1 hour at 4°C. The number of platelets bound with the cells was determined by the level of fluorescence in the cell lysate. (C) Anti-LOX-1 and anti-CD40L antibodies were added to the culture medium prior to the addition of platelets and levels were maintained throughout the experiments. Results are expressed as means ± SEM (n = 3); *P < 0.01. CHO, Chinese hamster ovary cells;MFI, mean fluorescence intensity.

LOX-1 antibody and anti-CD40L antibody. These results indicated that both LOX-1 and CD40 are involved in platelet–endothelium interaction (Fig. 1C).